



CENTER FOR INFRASTRUCTURE ENGINEERING STUDIES

OUT-OF-PLANE STATIC AND BLAST RESISTANCE OF UNREINFORCED MASONRY WALL CONNECTIONS STRENGTHENED WITH FIBER REINFORCED POLYMERS

by

Preston Carney

Dr. John J. Myers

University of Missouri-Rolla

CIES

03-46

Disclaimer

The contents of this report reflect the views of the author(s), who are responsible for the facts and the accuracy of information presented herein. This document is disseminated under the sponsorship of the Center for Infrastructure Engineering Studies (CIES), University of Missouri -Rolla, in the interest of information exchange. CIES assumes no liability for the contents or use thereof.

The mission of CIES is to provide leadership in research and education for solving society's problems affecting the nation's infrastructure systems. CIES is the primary conduit for communication among those on the UMR campus interested in infrastructure studies and provides coordination for collaborative efforts. CIES activities include interdisciplinary research and development with projects tailored to address needs of federal agencies, state agencies, and private industry as well as technology transfer and continuing/distance education to the engineering community and industry.

Center for Infrastructure Engineering Studies (CIES)

University of Missouri-Rolla
223 Engineering Research Lab
1870 Miner Circle
Rolla, MO 65409-0710
Tel: (573) 341-6223; fax -6215
E-mail: cies@umr.edu
www.cies.umr.edu

ABSTRACT

Recent world events have illustrated that sustainability of buildings to blast loads is an ever increasing issue. Many older buildings contain unreinforced masonry (URM) infill walls. Due to their low flexural capacity and their brittle mode of failure, these walls have a low resistance to out-of-plane loads, including a blast load. As a result, an effort has been undertaken to examine retrofit methods that are feasible to enhance their out-of-plane resistance. The use of externally bonded and near surface mounted (NSM) Fiber Reinforced Polymer (FRP) laminates and rods have been proven to increase the out-of-plane load capacity.

This research study investigated the feasibility of developing continuity between the FRP strengthening material and the surrounding reinforced concrete frame system. There were two phases to this research study. Phase I evaluated strengthened URM wall's out-of-plane performance using static tests. Two strengthening methods were utilized, including the application of glass FRP (GFRP) laminates to the wall's surface and the installation of near surface mounted (NSM) GFRP rods. In both methods, the strengthening material was anchored to boundary members above and below the wall on some of the specimens in the research program. A shear retrofit, the effects of bond pattern, and the effects of FRP laminate strip width were also investigated in this phase. Phase II involved the field blast testing of two walls to dynamically study the continuity detail for laminates and verify the results obtained in Phase I. The development of continuity between the FRP materials and the surrounding framing system is important to improving the blast resistance of URM infill walls.

ACKNOWLEDGMENTS

I would like to express my appreciation to my advisor Dr. John Myers for his guidance and assistance throughout this project. I would also like to thank my committee members Dr. Paul Worsey, for his expertise in the field of explosives, and Dr. Antonio Nanni, for his input throughout this project.

Special thanks also go to the technical support staff of the Department of Civil Engineering at the University of Missouri – Rolla (UMR). This includes Jason Cox, Steve Gabel, Jeff Bradshaw, Gary Abbot, and Bill Fredrickson. My sincere thanks also go to my friends who helped with the testing: William Bolte, Nick Ereckson, Matt Gebhardt, Randy Haffer, and Matt Swenty. Above all, this research would not have been possible without the help of Daniel Koenigsfeld, of whom I am greatly appreciative.

I would like to thank the National Science Foundation's Industry University Cooperative Research Center, the Repair of Buildings and Bridges with Composites (RB2C), for providing the funding for this project. My sincere thanks also go to Harold Martin of Rolla Technical Institute for constructing the walls, Randy Keller of International Paper's Ride Rite Division for providing the air bags, Dennis Hutchinson of Ft. Leonard Wood military base in St. Robert, Missouri for coordinating the field testing on base, Nestore Galati for providing assistance in calculating theoretical results, and to Hughes Brothers, Inc. for providing the GFRP rods used in this research.

Finally, I am extremely appreciative of the support my family has provided me throughout my college career. Thanks to my parents, Ronnie and Susan Carney, and my two brothers Brandon and Trenton Carney.

TABLE OF CONTENTS

	Page
ABSTRACT.....	iv
ACKNOWLEDGMENTS	v
LIST OF ILLUSTRATIONS.....	ix
LIST OF TABLES.....	xii
NOMENCLATURE	xiii
 SECTION	
1. INTRODUCTION.....	1
1.1. BACKGROUND	1
1.2. SCOPE AND OBJECTIVES.....	4
1.3. REPORT LAYOUT.....	4
2. REVIEW OF LITERATURE.....	6
2.1. MASONRY WALL TESTING	6
2.1.1 Out-of-Plane Load Testing.....	6
2.1.2. Testing of Walls Strengthened with FRP.....	9
2.2. CHARACTERISTICS OF EXPLOSIONS AND BLAST RESISTANT DESIGN	15
2.2.1. Characteristics of Explosions.....	15
2.2.2. Blast Resistant Design.....	18
3. FRP COMPOSITE SYSTEMS	21
3.1. MATERIAL PROPERTIES	21
3.2. STRENGTHENING TECHNIQUES.....	26
3.2.1. Laminate Manual Lay-up.....	26

3.2.2. Near Surface Mounted (NSM) Rods.....	27
4. EXPERIMENTAL PROGRAM.....	30
4.1. OUT-OF-PLANE LOAD TESTING.....	30
4.2. TEST MATRIX.....	32
4.3. CONSTRUCTION OF WALLS.....	34
4.4. TEST SETUP AND TESTING PROCEDURES – LAB.....	48
4.5. TEST SETUP AND TESTING PROCEDURES – FIELD.....	52
5. RESULTS AND DISCUSSION.....	56
5.1. LABORATORY RESULTS.....	56
5.1.1. Wall #1.....	56
5.1.2. Wall #2.....	56
5.1.3. Wall #3.....	58
5.1.4. Wall #4.....	59
5.1.5. Wall #5.....	61
5.1.6. Wall #6.....	61
5.1.7. Wall #7.....	62
5.1.8. Wall #8.....	62
5.1.9. Wall #9.....	63
5.1.10. Wall #10.....	64
5.1.11. Wall #11.....	67
5.1.12. Wall #12.....	67
5.2. FIELD RESULTS.....	69
5.2.1. Wall #1.....	69

5.2.2. Wall #2	70
5.3. DISCUSSION	72
6. CONCLUSIONS	85
6.1. CONCLUSIONS	85
6.2. FUTURE RECOMMENDATIONS	86
APPENDICES	
A TEST DATA	88
B. SAMPLE CALCULATIONS	109
BIBLIOGRAPHY	113

LIST OF ILLUSTRATIONS

Figure	Page
2.1. Arching Action Mechanism (Tumialan et al. 2000).....	7
2.2. Moment Capacity versus Reinforcement Index (Tumialan et al. 2003).....	13
2.3. Pressure vs. Time Profile	17
3.1. Testing of Concrete Cylinders	23
3.2. Casting of Mortar Cubes.....	24
3.3. Testing of Mortar Cubes	24
3.4. Masonry Prism.....	25
3.5. Testing of Masonry Prisms	25
3.6. Manual Wet Lay-up Process.....	28
3.7. Near Surface Mounting Process.....	29
4.1. Airbag Used for Loading	31
4.2. Formwork for Boundary Elements	35
4.3. Beam Detail, Steel Cages, and Forms.....	36
4.4. Pouring Concrete	37
4.5. Wall Construction.....	37
4.6. Supporting Frame.....	38
4.7. Grouted Bottom Course	39
4.8. Injected Foam.....	39
4.9. Grouted Top Course.....	40
4.10. Field Application Schematic.....	41

4.11. NSM Rod Anchorage.....	41
4.12. Predrilled Holes	41
4.13. Raked Head Joint	42
4.14. Raked Joint and Predrilled Hole	43
4.15. Anchored NSM Rod	43
4.16. Laminate Anchorage.....	44
4.17. Groove in Beam	44
4.18. Groove with Wall Constructed	45
4.19. Sheet Wrapped in Groove.....	46
4.20. Groove Filled with Paste.....	46
4.21. #2 GFRP Bar Inserted into Groove.....	47
4.22. Completed GFRP Laminate Anchorage System.....	47
4.23. Test Setup.....	49
4.24. Strain Gage Locations.....	50
4.25. Dial Gage Setup	51
4.26. Precise Ruler for Deflection Measurement.....	52
4.27. Frame and Boundary Setup.....	53
4.28. Phase II Test Setup.....	54
4.29. Suspension of Charge	55
5.1. Wall #1 Failure	57
5.2. Wall #2 Failure	58
5.3. Wall #3 Failure	60
5.4. Wall #4 Failure	61

5.5. Wall #5 Failure	62
5.6. Wall #7 Failure	63
5.7. Wall #8 Failure	64
5.8. Wall #9 Failure	65
5.9. Wall #10 Failure	66
5.10. Wall #11 Failure	68
5.11. Wall #12 Failure	69
5.12. Wall #1 Failure	71
5.13. Cracking.....	71
5.14. Damaged Wall	72
5.15. Wall #2 Failure	73
5.16. Peak Out-of-Plane Pressure Results for Phase I Test Walls at Failure.....	74
5.17. Pressure versus Displacement for Phase I Walls	75
5.18. Pressure versus Corrected Displacement.....	77
5.19. Normalized Strain Energy Ratio.....	78
5.20. Strengthening Scheme Effects on Normalized Ductility Ratio	79
5.21. Laminate Strip Width Effects on Normalized Ductility Ratio.....	80
5.22. Pressure Ratio versus Reinforcement Index	83

LIST OF TABLES

Table	Page
2.1. Summary of Results (Hamilton III and Dolan 2001).....	12
2.2. TNT Equivalent Conversion Factors (Mays 1995).....	18
3.1. Properties of GFRP Rebar (Hughes 2001).....	21
3.2. Properties of GFRP Fabric (Watson 2002b).....	22
3.3. Properties of Application Materials (¹ Watson 2002a, ² ChemRex [®] 2002).....	22
3.4. Mortar Strength.....	25
4.1. Experimental Test Matrix	35
4.2. Summary of Blast Events.....	55
5.1. Levels of Damage to Tested Walls (El-Domiaty et al. 2002).....	70
5.2. Summary of Blast Events and Levels of Failure	70
5.3. Summary of Failure Modes for Phase I.....	78
5.4. Equivalent Uniform Pressures	82
5.5. Theoretical Results.....	83

NOMENCLATURE

Symbol	Description	Page
h/t	Slenderness Ratio	6
h	Height of Wall	6
t	Thickness of Wall	6
w	Ultimate Uniform Load	9
f'_m	Masonry Compressive Strength	9
λ	Strength Factor	9
R_1	Reduction Factor	9
R_2	Reduction Factor	9
ε_{mu}	Masonry Compressive Strain Capacity	11
ε_{gu}	GFRP Tensile Strain Capacity	11
α_c	Coverage Ratio	11
b_g	Width of GFRP Strap	11
b	Effective Flange Width of Cross Section	11
f_{gu}	GFRP Capacity (force per unit width)	11
d	Effective Depth	12
a	Depth of Equivalent Stress Block	12
T_{gu}	Strap Capacity	12
M_n	Nominal Moment Capacity - Flexural Bending	12
c	Depth of Neutral Axis	12
ω_f	Reinforcement Index	13

ρ_f	Flexural Reinforcement Ratio	13
E_f	Modulus of Elasticity of FRP	13
t_a	Delayed Time	16
p_s	Peak Pressure.....	16
T_s	Duration of Positive Phase	16
p_o	Ambient Air Pressure	16
Z	Scaled Distance	16
R	Standoff Distance	16
W	Charge Weight.....	16
Q_x	Mass Specific Energy of an Explosive.....	17
Q_{TNT}	Mass Specific Energy of TNT	17
P_{so}	Peak Pressure.....	17
Q	Weight of Pentolite.....	17
f'_g	Grout Compressive Strength	24
E_g	Grout Modulus of Elasticity	76
u_f	Ultimate Deflection	77
u_y	Deflection at Apparent Yield Point	77
V	Maximum Shear	110
M	Maximum Moment.....	110
w	Applied Uniform Load	110
w'	Equivalent Uniform Load.....	110
p	Applied Pressure.....	111
p'	Equivalent Uniform Pressure	111

1. INTRODUCTION

1.1. BACKGROUND

Recent events throughout the world have drawn attention to the vulnerability and sustainability of buildings and infrastructure to acts of terrorism. Our infrastructure is vital to this nation's economy and way of life. Any damage to it would and has had drastic effects on our culture. Attacks may cause a variety of results ranging from minor building damage to complete structural failure and considerable loss of life. Some examples within the United States include the bombing of the Murrah Federal Building in Oklahoma City (1995) and the bombing and attacks on the World Trade Center in New York City (1993, 2001). Abroad, numerous attacks have been directed toward embassies, and suicide car bombers have been used to target populated areas. In the cases where complete structural failure is not an issue, the dangers of flying debris have resulted in loss of life or injury to numerous civilians. Of particular concern are unreinforced masonry (URM) infill walls. Structural systems composed of a reinforced concrete (RC) framing system with URM infill walls makes up a significant portion of the building inventory in the United States and around the world. Since there is no reinforcement within these walls, they have little resistance to out-of-plane loads such as a blast load. As a result, an effort has been undertaken to examine retrofit methods that are feasible to enhance their out-of-plane resistance. One method of strengthening URM walls is the application of fiber reinforced polymers (FRP) to the surface of the wall to improve their performance.

Today, FRP is considered an emerging technology. Its use began becoming more widespread following World War II when the aerospace industry began to make use of its

unique properties. FRP was a material that could have a very high strength, but was still lightweight, making it an ideal material for use in this industry. Following this, the use of FRP became even more widespread as it was used in the manufacturing of golf clubs and fishing poles, and in the 1960s FRP was considered for use in reinforced concrete as concerns of rebar corrosion began to escalate. Epoxy coated rebar became the acceptable solution at the time, but in the 1990s the long-term effectiveness of epoxy coated bars began to be questioned. As a result, FRP is being considered as a long-term solution (ACI 440.1R-01).

Not only can FRP be used within concrete, but it also can be applied to the surface. Externally bonded FRP systems have been investigated and been used since the 1980s. External bonding is a developing technology and has been used to strengthen a wide variety of structural systems and members. Externally bonded FRP may be applied to more than just concrete. Other materials that have been strengthened include wood, steel, and masonry. External bonding of FRP was first used as an alternate to bonding steel to the surface of a material. These FRP systems can be applied to concrete columns to provide additional confinement or applied to beams for flexural or shear strengthening (ACI 440.2R-02).

Since the effects of a blast cause a pressure to be exerted on the surface of a wall, the flexural behavior of the wall can be observed. This makes it appropriate to strengthen the walls to improve their flexural capacity. The application of externally bonded FRP materials have been shown to improve the flexural capacity of walls with and without arching action (El-Domiaty et al. 2002), but the development of continuity between the wall system and surrounding boundary members needs to be investigated.

Strengthening of walls is not the only step involved in the process of reducing a building's vulnerability to blast loadings. Proper risk assessment must also be performed to determine the level of vulnerability of a structure. One must also determine the level of damage that is acceptable for the structure to sustain. The characteristics of an explosion are key in assessing this vulnerability. The pressures that are developed as a result of an explosion are a function of the weight of the charge and the distance from the explosion, commonly called the standoff distance. The charge weight is expressed in terms of equivalent weight of trinitrotoluene (TNT). As you increase the charge weight the pressures that are developed are also increased. Similarly, as the standoff decreases, the pressures on a surface increase. For a given charge weight, the effects may be drastically different if the standoff distance is changed. For a very small standoff distance, strengthening the wall per se may have little effect; rather the addition of significant mass in the form of thick walls is often the approach. However, it may be more appropriate to try to increase the standoff distance to a facility by implementing barriers or restricting vehicular access to a structure. Wall strengthening would then allow for a compromise, that is the standoff distance would only have to be increased to the point which the strengthened wall could withstand the pressure from the design blast. With the proper assessment and an understanding of the key parameters, the strengthening of URM infill walls with FRP to improve their blast resistance has great potential.

1.2. SCOPE AND OBJECTIVES

Previous research that is described later in Section 2 has shown that externally mounted FRP has improved the out-of-plane performance of URM infill walls. This research investigation further investigates the ability of FRP to increase the flexural capacity and ductility of URM infill walls. There are several retrofit techniques that have been investigated in this research program.

The first technique was the application of FRP laminates and near surface mounted (NSM) FRP rods to the surface of the wall to increase the flexural capacity of the walls. The FRP was anchored to the surrounding boundary members for the purpose of developing continuity between the wall system and the surrounding RC framing system. A shear retrofit technique was also observed in an attempt to improve the shear capacity of the masonry in the regions near the boundary members. The effects of bond pattern, stacked versus running bond, were also observed in this research program to examine any impact on the out-of-plane strength of the walls. These out-of-plane tests were performed in the laboratory under static loading conditions using an air bag as the loading mechanism. These tests evaluated the effectiveness of anchoring the FRP material to the boundary members for development of continuity. Field blast testing was performed on two wall systems to evaluate the retrofit scheme that was most effective under out-of-plane loading in the lab.

1.3. REPORT LAYOUT

This report is organized in the following manner. Section one discusses the objectives and scope of the research program, as well as its significance. Section two

describes previous work related to out-of-plane testing of URM masonry infill walls and strengthening techniques that have been used for masonry systems. This section also introduces the characteristics of explosions. The third section describes the materials used in the project and their mechanical properties. The two FRP retrofit techniques are also described in this section. Section four describes the experimental program, including the test matrix and the experimental test setup. The results of the test program are presented in section five, along with the analysis and discussion. Finally, section six presents the findings of the research study and offers recommendations on future work in the area of blast resistance of URM infill walls.

2. REVIEW OF LITERATURE

2.1. MASONRY WALL TESTING

Masonry has been around for years and has been the primary building material for a large number of buildings, both government and commercial structures, throughout the world. As a result of its widespread use, there has been a vast amount of research conducted in this area. Testing in the in-plane direction of reinforced and unreinforced masonry walls has been the focus of many research programs to evaluate the walls' behavior under lateral loading including seismic events. Significant work has also evaluated the out-of-plane performance of masonry wall systems including URM infill walls. This work includes both URM walls and walls that have been strengthened with bonded FRP laminates and NSM FRP rods.

2.1.1 Out-of-Plane Load Testing. Previous work has been performed on URM infill walls. This includes research on quarter scale masonry walls and methods to predict the out-of-plane strength of a masonry wall when arching action is present. Arching action is a phenomenon that may occur in a masonry wall based on a given wall's slenderness ratio (h/t). The effects of arching on a wall can be considered small if the slenderness ratio is larger than 30 (Angel et al. 1994). An infill wall exhibiting arching action first undergoes cracking at midspan when an out-of-plane load is applied to the wall. Three hinges are then formed. One occurs at midspan and one at each of the supports. The upper and lower halves of the wall then begin to rotate as a rigid body. No flexural bending can be observed when arching action is present. As the load increases, further rotation occurs, causing a compressive force to be exerted in the plane of the wall.

A shear force is also developed at the support locations (Tumialan 2001). Figure 2.1 illustrates the arching action mechanism.

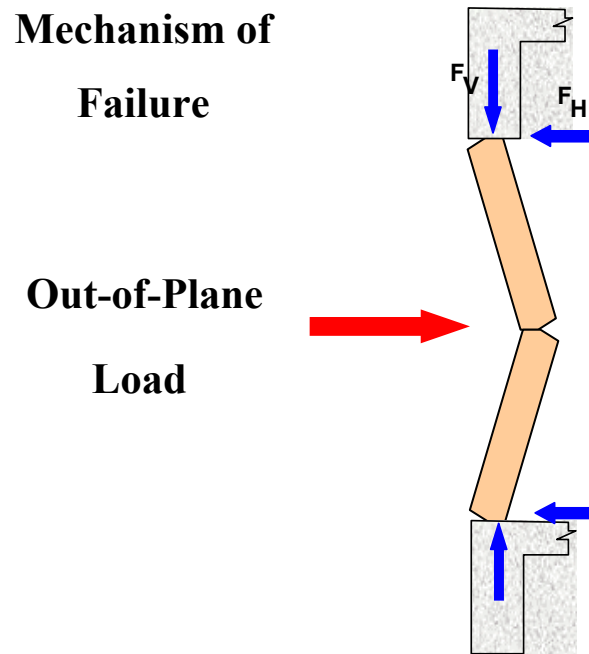


Figure 2.1. Arching Action Mechanism (Tumialan et al. 2000)

Within a RC framed buildings there are some constructability issues associated with the development of arching action. The development of arching action is dependant upon the transfer of force to the boundary member above the wall. When a wall is constructed within a RC frame, it is difficult to place mortar between the top of the wall and the top boundary member. Research has been performed on this topic related to earthquake motions. Specimens were constructed with a complete mortar joint and some with partially filled mortar joints. The walls were 9.8 ft (3 m) wide x 11.5 ft (3.5 m) tall

x 9.4 in (24 cm) thick constructed using double wythe, unreinforced bricks. This results in a slenderness ratio of about 15. Sand limestone bricks were used, having dimensions of 9.4 in x 4.5 in x 4.4 in (240 mm x 115 mm x 113mm). The walls were subjected to a seismic simulation using a shake table. Arching action was present and no significant difference was noticed in the behavior of the wall with the complete joint and the wall with the partially filled joint (Dafnis et al. 2002).

The response of masonry walls to blast loading has been studied in the form of walls constructed out of 1/4-scale concrete masonry units (CMU). This research was used to validate a computer model developed to predict the response of masonry walls which undergo blast loading. The walls in this study were ungrouted, unreinforced, one-way wall systems. They were studied both statically and dynamically. The static tests were performed in a frame, using water to load the test specimen. A 32 inch (812.8 mm) high by 64 (1625.6 mm) inch wide wall was constructed of 1/4-scale 8 x 8 x 16 inch (203.2 x 203.2 x 406.4 mm) CMU in the frame in which water can be contained on both sides of the wall. Water was placed in the structure on both sides of the wall. After the water level was above the surface of the wall, one side was pressurized slowly until failure. The wall failed under a static load of 8.5 psi (58.6 kPa). Field blast tests were also performed and compared to computer models in this research program (Dennis et al. 2002).

Significant work has also been performed in an attempt to estimate the out-of-plane strength of URM infill walls. The goal of this research was to develop an equation to predict the strength of infill walls that have been cracked and to account for the stiffness of the surrounding frame. The test setup for this experiment involved the

construction of a URM wall within a RC frame to simulate the actual framing system that would typically be seen in a RC frame type building. An airbag was used to apply a uniform load to the wall. From the results, the following equation was developed to predict the ultimate uniform load, w , that can be applied to the infill. f'_m is the

$$w = \frac{2f'_m}{h/t} R_1 R_2 \lambda \quad (\text{Equation 2.1})$$

compressive strength of the masonry and h/t is the slenderness ratio of the infill wall. λ is a strength factor that varies with the slenderness ratio. R_1 and R_2 are both reduction factors developed to account for cracking and frame stiffness, respectively (Shapiro et al. 1994). Using this equation, one can estimate the strength of a given infill wall. If the expected loading exceeds the strength, it may be necessary to strengthen the walls to increase their capacity.

2.1.2. Testing of Walls Strengthened with FRP. One method for strengthening URM walls that has been studied in depth is the application of FRP materials to the surface of the walls to improve their performance. Due to recent research, strengthening of URM walls in the out-of-plane direction is becoming a more well developed method. However, more research is needed to better define the design methods and to develop alternatives to further improve a wall's performance.

Several research programs have investigated out-of-plane performance under simply supported conditions. In one research program, FRP in various types, amounts, and layouts was applied vertically to 13.1 ft (4 m) tall by 3.9 ft (1.2 m) wide by 7.5 in (0.19m) thick walls. Both metric and imperial dimension blocks were used in this research, so the wall dimensions vary slightly, depending on which type of block was used for their construction. The wall panels were loaded using a hydraulic jack, and two

line loads offset from midspan were applied. The walls were simply supported, so no arching action was present. From the test results, three failure modes were determined to control this test program. These include flexure, flexure-shear, and mortar separation. The effects of axial load and cyclic behavior were also evaluated. The maximum load applied to the unstrengthened wall was 225 lb (1.0 kN). It was concluded that strength of the wall was significantly improved by the application of FRP, as was the ductility of the wall system. The capacity was improved to an average of 7.9 k (35 kN) depending on reinforcement amounts and configurations, as well as boundary conditions. An analytical model was also developed. It was proven to be effective in the prediction of transition level loads and deflections. However, the model's correlation to ultimate strength and deflections was not accurate (Albert et al. 2001).

A similar research program investigated the application of Glass FRP (GFRP) to clay bricks. This study also used simply supported conditions. The load, however, was applied by an air bag to develop a uniform load on the wall. Both sides of the walls were strengthened and cyclic loading was used. Delamination of the composites and high shear stresses controlled the failure. This research again showed increased strength and deflection capacity. The researchers also determined that it appeared there was a direct relationship between the reinforcement ratio and the load at initial cracking, delamination, and ultimate strength (Velazquez-Dimas et al. 2000).

In research performed by Hamoush et al., fifteen 48 in (1219 mm) x 72 in (1829 mm) x 8 in (203 mm) wall panels were investigated. Two reinforcement methods were used in this research. They include the use of two layers of continuous FRP webbing and vertical and horizontal strips of unidirectional FRP which cover the majority of the wall.

Two surface preparation techniques were also examined. These include wire brushing the surface and sandblasting. Again, simply supported conditions were used. Uniform loading was achieved by using an air bag loading system. The unreinforced samples failed due to flexure. With one exception, all of the strengthened walls failed in shear. This work illustrated that shear can control the failure of URM walls and an attempt to control the shear should be made to be able to achieve the full flexural strength. Both the wire brushing and the sand blasting produced a sufficient bond. The continuous FRP webbing covering the entire wall produced only slightly higher strengths over the use of the strips. The flexural performance was improved from 0.14 psi (1 kPa) for the unreinforced case to an average of 2.9 psi (20 kPa) for the strengthened walls (Hamoush et al. 2001).

Work on the out-of-plane strength of URM walls has also been performed at the University of Wyoming. This research also used an air bag loading system and simply supported conditions. Their primary failure modes include the rupture of the GFRP and a combined delamination and rupture. Both short [24 in (610 mm) x 72 in (1800 mm) x 8 in (200 mm)] and tall [48 in (1220 mm) x 184 in (4700 mm) x 8 in (200 mm)] walls were used in this study. Their results are summarized in Table 2.1. This experimentation also led to the development of equations to predict the capacity of simply supported walls. These equations are as follows:

Balanced Condition

$$\alpha_c = b_g / b = (0.85)^2 t \frac{f'_m}{f_{gu}} \left(\frac{\epsilon_{mu}}{\epsilon_{mu} + \epsilon_{gu}} \right) \quad (\text{Equation 2.2})$$

Table 2.1. Summary of Results (Hamilton III and Dolan 2001)

Height	Specimen	CMU	Capacity [kPa (psf)]	Failure Mode
Short	1	Normal Weight	15.0 (313)	Delamination
	2	Normal Weight	18.4 (384)	GFRP Rupture/ Delamination
	3	Lightweight	21.3 (445)	GFRP Rupture
	4	Lightweight	23.7 (495)	GFRP Rupture/ Delamination
Tall	1	Lightweight	5.9 (124)	GFRP Rupture/ Delamination
	2	Lightweight	4.8 (100)	GFRP Rupture

Underreinforced Condition

$$M_n = T_{gu}(d - a / 2) \quad (\text{Equation 2.3})$$

Where

$$a = \frac{T_{gu}}{.85 f'_m b} \quad (\text{Equation 2.4})$$

$$T_{gu} = b_g f_{gu} \quad (\text{Equation 2.5})$$

Overreinforced Condition

$$M_n = .85 a b f'_m (c / 2) \quad (\text{Equation 2.6})$$

The equations are similar to those used in reinforced masonry design, but they over predict the ultimate capacity. This over prediction does not exceed 20%, however more experimentation is required to validate the equations and develop an accurate reduction factor (Hamilton III and Dolan 2001).

Several research investigations have been undertaken at the University of Missouri – Rolla (UMR) involving URM wall panels. One program examined the use of FRP laminates and NSM rods applied to wall panels. These panels were tested under

simply supported conditions. The effects of first applying putty to a wall to which laminates were to be applied was also investigated and shown to improve the bond strength (Galati et al. 2003a). Design equations were also presented based on this research and other tests performed at UMR. It is suggested that the mode of failure and the flexural capacity are a function of a parameter called the reinforcement index (ω_f) as

$$\omega_f = \frac{\rho_f E_f}{f'_m (h/t_m)} \quad (\text{Equation 2.7})$$

illustrated in Figure 2.2. The parameters include ρ_f , the flexural reinforcement ratio, E_f , the modulus of elasticity of the FRP, f'_m , the compressive strength of the masonry, and h/t_m , the slenderness ratio of the wall (Tumialan et al. 2003).

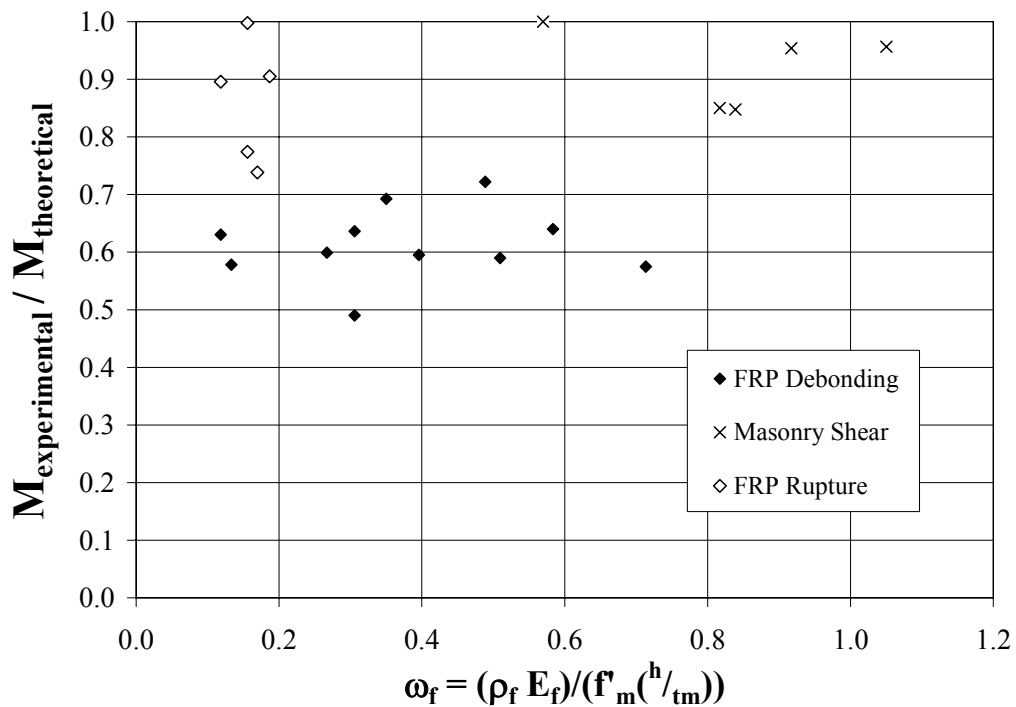


Figure 2.2. Moment Capacity versus Reinforcement Index (Tumialan et al. 2003)

Wall panels exhibiting arching action have also been investigated. It was shown that the additional capacity provided by the FRP is less in the case where arching is present than the simply supported condition (Galati et al. 2002). To prove the effectiveness of retrofitting existing URM infill walls, testing was performed at the Malcolm Bliss Hospital in St. Louis, Missouri prior to its demolition. This research was important to evaluate the effects of actual boundary conditions on the development of arching action and the effectiveness of strengthening techniques. The walls were tested using a point load. Anchorage techniques were used in this program, however due to the mode of failure for the case of the laminates and possible weakening of the walls during the installation in the case of the NSM rods, their performance could not be evaluated (Tumialan 2001).

This research program continues to build on the work performed by El-Domiatiy, Myers, and Belarbi (2002) at UMR. This work involved the field blast testing of URM walls. This work made use of three reinforcement schemes. The first was the application of vertical GFRP laminates along the bed joints of the masonry. The second was the use of NSM GFRP rods embedded in the bed joints. Finally, a hybrid system was used. This involved horizontal NSM FRP rods in the bed joints and vertical GFRP laminates along the head joints. Two wall sizes were used in this research program. They were 48 in (1219 mm) wide x 88 in (2235 mm) tall x 4 in (102 mm) thick and 48 in (1219 mm) wide x 88 in (2235 mm) tall x 8 in (203 mm) thick. Concrete boundary members were used above and below the wall, which allowed arching action to occur in the 8 in (203 mm) thick walls. No anchorage or continuity was developed between the boundary members

and the strengthening material. The strengthening schemes were effective, but a shear failure was experienced in a portion of the specimens (El-Domiaty et al. 2002).

It has been proven that FRP is effective in improving the out-of-plane strength of URM walls. The development of continuity between boundary members and the strengthening material needs to be investigated. Further capacity may be gained by anchoring the composites and result in more desirable failure modes with less debris scatter in the case of a blast. Shear problems have occurred in several of the research programs that have been discussed. An attempt should be made to control a failure due to shear near the boundary conditions. This research program investigated these issues in an attempt to improve URM infill wall's resistance to blast loads and extreme static out-of-plane loading.

2.2. CHARACTERISTICS OF EXPLOSIONS AND BLAST RESISTANT DESIGN

2.2.1. Characteristics of Explosions. To understand the effects of a blast on a building, one must have an understanding of the characteristics of an explosion. Explosions can be of three different types. These include chemical, nuclear, or physical explosions. Historically the explosives that are used in a terrorist act are typically of the chemical type.

A chemical explosion involves the rapid oxidation of the explosive's fuel elements. The components of the explosive contain the oxygen necessary for this reaction to occur. Therefore, it is not necessary for the explosive to have air available to it to detonate. Another key aspect of these explosives are their ability to be detonated on demand, while at the same time they are a stable material that can be easily transported

with little risk of accidental initiation. The most commonly used explosives are in the condensed form, either solids or liquids. When initiated, the explosive begins to react, producing heat and gas. The rapid expansion of the gas is responsible for the development of blast waves which cause a force to be exerted on structures.

When an explosive material is detonated, the blast wave begins at the source of the explosion and propagates outward in the radial direction. When the blast wave reaches a given location at a delayed time, t_a , the pressure increases to a peak value, p_s . With time, T_s , this pressure decays back to ambient air pressure, p_o . This phase of the blast wave is called the positive phase. The pressure continues to drop below ambient air pressure in the negative phase. This is illustrated in Figure 2.3. The area under the pressure versus time plot is defined as the impulse. While the curve illustrates the peak pressures that are developed, the impulse quantifies the duration of the load. The pressure time profile is a characteristic of a given explosive, so this must be taken into account when designing blast resistant structures.

The peak pressures developed from an explosion are critical in determining the effects on structures. The peak pressures are a function of a scaled distance. This scaled distance, Z , is calculated by dividing the standoff distance, R , by the cube root of the charge weight, W , as illustrated in Equation 2.8. The standoff distance is the distance

$$Z = R / W^{1/3} \quad (\text{Equation 2.8})$$

from the source of the explosion to the location at which the peak pressure is desired. Increasing this distance is the most effective way of reducing the effects of an explosion as will be discussed in the next section. The charge weight is the actual weight of material that is initiated. This weight is in terms of equivalent weight of TNT. Since

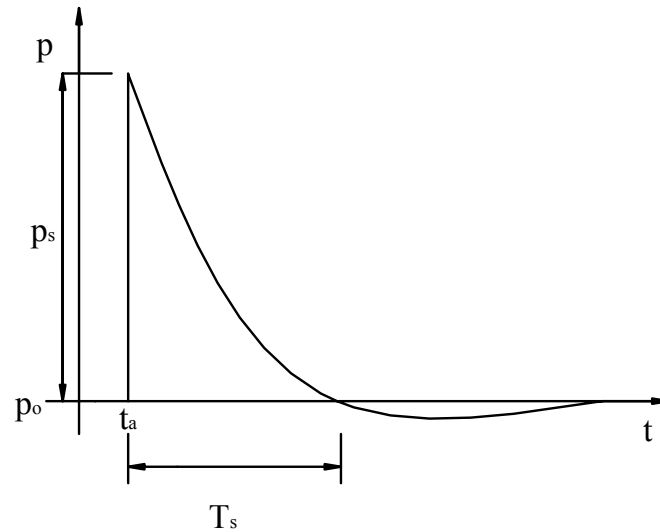


Figure 2.3. Pressure vs. Time Profile

there are numerous explosive materials available, it is necessary to convert the weight of each to an equivalent weight of TNT. This is obtained by taking the ratios of the mass specific energy of a given explosive, Q_x , to that of TNT, Q_{TNT} . Table 2.2 shows some conversion factors to convert to an equivalent weight of TNT (Mays 1995). El-Domiatty et al. (2002) developed the following empirical equation for the peak pressure, P_{so} (psi), in terms of charge weight of Pentolite, Q (lb), and standoff distance, R (ft).

$$P_{so} = 6670QR^{-2.5} \quad (\text{Equation 2.9})$$

With the standoff distance and the equivalent mass of an explosive material, one can calculate the peak pressure and the impulse related to a given explosion. The peak pressure is also related to the reflected overpressure that is exerted on a wall that is perpendicular to the blast wave. Given this information, one can perform a dynamic analysis to evaluate a building's performance under a blast load (Mays 1995).

Table 2.2. TNT Equivalent Conversion Factors (Mays 1995)

Explosive	TNT Equivalent (Q_x/Q_{TNT})
Compound B (60% RDX, 40% TNT)	1.148
RDX	1.185
HMX	1.256
Nitroglycerin (liquid)	1.451
TNT	1.000
Blasting Gelatin	1.000
60% Nitroglycerin Dynamite	0.600
Semtex	1.250

2.2.2. Blast Resistant Design. Blast resistant design has been practiced by the military for many years, but has been impractical for the design of commercial facilities. Most structures designed to resist blast loads have been underground facilities. Building these facilities below ground eliminates the need to design the walls for reflected overpressures. These overpressures are far greater than other lateral loads that buildings are designed for, drastically increasing the cost of construction. Another reason that has made it impractical to design structures for blast resistance is the inability to define the risk. It is not known what buildings will be targeted or when an attack will occur. Finally, it is very difficult to quantify the threat. There are many different materials that can be used to cause damage. Various weights of explosives can also be used (Longinow 1996). This illustrates the need for proper assessment as the first step in blast resistant design.

The risk associated with military facilities and embassies can be better estimated than that of commercial buildings. The military facilities have a specific purpose, and therefore their risk can be better evaluated. New embassy buildings must also conform to a design standard that accounts for acts of terrorism. Embassies are designed to prevent overall structural failure and loss of life. In military facilities, special consideration is given to maintaining the facilities purpose. In either case, there is typically a significant amount of free space surrounding the buildings. This is not the case for most commercial buildings. The free space is a critical design parameter for blast resistance (Ettouney 1996).

The free space surrounding a building is a key parameter in determining the scaled distance of an explosion. This space can be used in an efficient manner to increase the standoff distance. This would prevent the ability to transport large quantities of explosive materials to a location of close proximity to a building. This would drastically reduce the effects of the explosion on the structure, should it detonate. A set of guidelines for perimeter security has been developed. These guidelines state that the perimeter should be located at the maximum feasible distance, preferably a distance such that the design explosion will not induce structural damage on the building. The perimeter should also be of such structure as to prevent those unauthorized from gaining access. It should be visible from the building and be well lit so any increased activity near the perimeter can be easily noticed. Finally, it is suggested that a barrier be made of a combination of materials with redundancy. These may include fences, ditches, walls, embankments, or large planters (Longinow 1996).

When facilities do not have sufficient free space around them to establish an effective perimeter system, alternate methods should be investigated. This is also the case for buildings in urban areas. The application of FRP to the surface of URM infill walls may be an effective solution both in terms of improved resistance and debris scatter. The additional strength provided by the FRP material may reduce the necessary perimeter distance, making the blast resistant retrofit more feasible.

3. FRP COMPOSITE SYSTEMS

This research program made use of two FRP composite strengthening systems. The systems were laminate manual lay-up and near surface mounted (NSM) rods. Both systems use E-glass based fibers. The strengthening techniques will be discussed in detail within this section, as well as a description of the materials used in their application.

3.1. MATERIAL PROPERTIES

Fiber Reinforced Polymers are composite materials. To obtain full composite action, the glass fibers must be embedded in a resin. In the case of the GFRP rods, they are produced as a composite. The laminates, however, are produced as dry fibers. They are embedded in a resin as they are applied to the surface. The rods and glass fiber sheets are responsible for the strength increase of the structure to which they are applied. The GFRP rods used in this research are size #2 and their properties as indicated by their manufacturer are indicated in Table 3.1. The laminates are made of unidirectional fibers of E-glass. The fabric's properties shown in Table 3.2 have been determined by the manufacturer.

Table 3.1. Properties of GFRP Rebar (Hughes 2001)

Bar Size	Cross Sectional Area (in ²)	Nominal Diameter (in)	Tensile Strength (ksi)	Tensile Modulus of Elasticity (ksi)
#2	.0515	.25	120	5920

Conversions: 1 in = 25.4 mm, 1 in² = 645.2 mm², 1 ksi = 6.895 MPa

Table 3.2. Properties of GFRP Fabric (Watson 2002b)

Nominal Thickness (in)	Ultimate Tensile Strength (ksi)	Tensile Modulus of Elasticity (ksi)	Ultimate Rupture Strain	Ultimate Tensile Strength per Unit Width (k/in)
.0139	220	10500	2.1%	3.06

Conversions: 1 in = 25.4 mm, 1 ksi = 6.895 MPa, 1 k/in = .175 kN/mm

The application of GFRP laminates or sheets involves several other materials to be discussed in detail later in this section. The materials used include a primer, putty, and a saturant. The NSM rods are applied to the walls using a paste. The material properties of the substances used to apply the fibers to the wall are listed in Table 3.3, as provide by the manufacturer.

The walls used in this research program are constructed from blocks produced by a local producer of concrete masonry units (CMU) in central Missouri. Concrete

Table 3.3. Properties of Application Materials (¹Watson 2002a, ²ChemRex[®] 2002)

	Primer ¹	Putty ¹	Saturant ¹	Paste ²
Tensile Strength (psi)	2500	2200	8000	4000
Tensile Strain	.40	.06	.03	.01
Tensile Modulus (psi)	104,000	260,000	440,000	-
Poisson's Ratio	.48	.48	.40	-
Compressive Strength (psi)	4100	3300	12,500	12,500
Compressive Strain	.10	.10	.05	-
Compressive Modulus (psi)	97,000	156,000	380,000	450,000

Conversion: 1 psi = 6.895 kPa

boundary members were cast in the High-Bay Structural Engineering Research Laboratory (SERL) in Butler-Carlton Civil Engineering Hall at UMR. Cylinders were cast according to ASTM specification C 31-00. The cylinders were tested according to ASTM C 39-01. Neoprene bearing pads were used in this test. The boundary members were cast in two pours using reusable forms as shown later in Section 4.3. The first group had a compressive strength of 3300 psi at the time the first series of walls were tested while the second group had a compressive strength of about 4000 psi also at the time of the tests. The cylinders used for the compressive test were field cured with the boundary elements. Figure 3.1 illustrates the compression testing of the standard 4 in x 8 in (101.6 mm x 203.2 mm) cylinders.

Mortar mix was used in the joints in the construction of the infill masonry walls. A premixed combination of masonry cement and fine graded sand was used. This mix conforms to ASTM C 387-00 type N mortar. To verify this, 2 in (50.8 mm) mortar cubes were cast and tested the as illustrated in Figure 3.2 and 3.3 respectively according to ASTM C 109-02. The mortar cubes were moist cured until testing. The testing revealed



Figure 3.1. Testing of Concrete Cylinders



Figure 3.2. Casting of Mortar Cubes



Figure 3.3. Testing of Mortar Cubes

that the mortar, or grout, was above the minimum strength required by the specification. Table 3.4 summarizes the grout compressive strength, f'_g , for the walls. The strength indicated in the table is the average of three cube tests. Finally, as seen in Figure 3.4, masonry prisms were constructed to determine the field cured compressive strength of the masonry. The tests were conducted according to ASTM C 1314-02a without capping and with slight modification to the test apparatus. This is illustrated in Figure 3.5. The

Table 3.4. Mortar Strength

	Walls	f'_g (psi)
Phase I	Series I	2000
	Series II	1150
Phase II	-	1250

Conversion: 1 psi = 6.895 kPa



Figure 3.4. Masonry Prism



Figure 3.5. Testing of Masonry Prisms

compressive strength of the masonry was determined to be about 1350 psi (9308 kPa). The strength of the masonry is a key parameter in determining out-of-plane strength, as well as the reinforcement index as discussed in the previous section. After the construction of the walls, the FRP was applied to them using the two techniques.

3.2. STRENGTHENING TECHNIQUES

3.2.1. Laminate Manual Lay-up. The GFRP laminates used in this research program rely on the establishment of a bond between the fiber and the surface of the wall. This bond is created by the application of a primer, putty, and saturant. The manufacture's recommended installation procedure was followed for this application. The surface of the masonry should be clean before beginning the manual wet lay-up process, but sandblasting is not required.

The first step is the application of primer to the area where the fibers were applied (Figure 3.6a). The primer is an epoxy based material designed to penetrate the pores in the concrete block. This step is necessary to provide a good surface to bond the rest of the application system to the CMU. Following the primer, a putty was applied to the surface as required (Figure 3.6b). The putty's purpose is to fill in any irregularities on the surface and to provide a smooth level surface to which the fibers bond. Next, the saturant was applied to the wall (Figure 3.6c). The saturant is the material that the glass fibers are embedded within to form the FRP composite. After the saturant was applied to the wall, the glass fibers were "laid up" (Figure 3.6d). A hard plastic roller with small prongs was used to roll the fibers in place. This was to assure proper wetting of the fibers. Wetting, or the saturation of the fibers, is essential in forming the FRP composite. After the glass

sheet was in place, another layer of saturant was applied (Figure 3.6e). Again, the pronged roller was used to help the saturant penetrate the fibers.

3.2.2. Near Surface Mounted (NSM) Rods. Near surface mounting of GFRP rods involves the installation of GFRP rebar within the vertical mortar joints in the walls. #2 GFRP rebar was used for this process. The size of existing mortar joints provides a size limitation as to which bars can be used. A #2 bar fits within the head joints, leaving enough room for epoxy. To install the GFRP rods within the joints, it is first necessary to grind out the mortar joints (Figure 3.7a). The mortar should be ground out to a depth of about 3/8 to 1/2 in (9.5 to 12.7 mm). The wall should be thoroughly cleaned after the grinding of the joints. The groove in the mortar joints is then filled with an epoxy based paste (Figure 3.7b). The GFRP rods are then inserted into the groove (Figure 3.7c). Additional paste is applied if necessary to completely surround the rod. The paste is leveled off with the surface of the wall, completing the installation process (Figure 3.7d).

These two FRP installation methods were utilized within this research program. In both cases, the FRP was anchored to boundary members. The anchorage techniques will be described in a later section. The use of proper material and installation techniques is essential in establishing proper bond and composite action.



(a) Application of Primer



(b) Application of Putty



(c) Application of Saturant



(d) Lay-up of Fibers



(e) Application of Second Layer of Saturant

Figure 3.6. Manual Wet Lay-up Process



(a) Groove in Vertical Joint



(b) Fill Joint with Paste



(c) Insert GFRP Bar



(d) Level Surface

Figure 3.7. Near Surface Mounting Process

4. EXPERIMENTAL PROGRAM

This section provides information and details of the experimental program used in this research study. A brief description of out-of-plane load testing will be provided and the development of the test matrix will be discussed. The process of constructing the walls will be detailed step by step. To conclude the section, a detailed explanation of the test setup and testing procedures is provided.

4.1. OUT-OF-PLANE LOAD TESTING

The testing of URM walls in the out-of-plane direction can be accomplished in a variety of ways. Testing for seismic resistance can be done by constructing a wall on a shake table and inducing a cyclic motion causing a dynamic load to be exerted on the wall. Static tests can also be performed to evaluate the out-of-plane performance of a wall.

Several different methods of loading have been utilized in previous research to effectively apply a static load. Some research programs have applied a point load either at center span or used a device to apply two point, or line, loads on either side of the midpoint of the wall. Sometimes, point loads are not an effective loading mechanism when evaluating a wall's performance. It may be necessary to attempt to apply a uniform load over the entire surface of the wall.

A complex, but effective method of applying a uniform load is the use of a pressurized water chamber. A wall can be constructed between two tanks and one of them pressurized to apply a uniform load to the wall. A simpler method is the use of an airbag. An airbag can be used to apply a load by placing the bag in contact with the test

wall and a reaction structure. As the pressure in the bag increases, the load on the wall also increases. This loading mechanism was utilized in Phase I of this research program to obtain a more uniform load on the wall. Blast loads are applied through an increase in the air pressure at the face of the wall causing a well distributed load. Therefore, an attempt should be made to apply a uniform load to evaluate a wall's performance for blast resistance when a static load is applied. Phase II used an actual blast event to create the loading for the test walls.

The airbag used in this research program had deflated dimensions of 36 in (914.4 mm) wide by 48 in (1219.2 mm) tall. They are six ply paper dunnage bags commercially produced by International Paper's Ride Rite Division. They are capable of withstanding pressures of over 20 psi (138 kPa) according to their representative, based on testing by the manufacturer. Figure 4.1 illustrates the bag utilized in this project. A special air chuck is needed to fill the bags. Within the fill port there is a one way air valve. This



Figure 4.1. Airbag Used for Loading

valve was removed for this research program to allow the pressure in the bag to be measured. More details of the instrumentation are provided in the test setup section.

4.2. TEST MATRIX

The development of this test program was based on previous research performed at UMR (El-Domiaty et al. 2002). The previous work illustrated that strengthening masonry walls with FRP materials does in fact improve their out-of-plane performance. This research will further investigate the effectiveness of strengthening URM walls with several variables.

The research performed by El-Domiaty et al. identified a shear problem in the course of blocks near the boundary members under blast loads. As a result of this failure mode, this program included a shear retrofit technique that could be used in-situ. Previous research has not evaluated the development of continuity between the FRP strengthening material and the boundary elements. This research program evaluated the effectiveness of the application of both GFRP laminates and NSM rods to URM walls with top and bottom boundary members. The focus of the research was the anchorage of the FRP to these boundaries. The effects of varying the laminate strip width and CMU bond pattern was also investigated.

This research was completed in two phases. Phase I was the evaluation of the retrofit techniques under static loading conditions using an airbag to incrementally load the walls. Phase I was divided into two series. Series I consisted of six test walls. Series II is composed of an additional six walls based on the results obtained from Series I. Phase II was the field evaluation of two walls under actual blast loading. The walls in

both phases were constructed of 4 in x 8 in x 12 in (101.6mm x 203.2 mm x 304.8 mm) CMU. The overall dimensions of the walls were 48 in (1219.2 mm) tall by 36 in (914.4 mm) wide. The 36 in (914.4 mm) wide dimension allowed for the wall to be three blocks wide giving two vertical, or head, joints in each wall. The FRP was applied along or within each of the head joints.

Consideration to previous work was given when developing the experimental program for Series I. This series consisted of two different retrofit schemes and a control wall. A duplicate of each wall was constructed with a possible shear retrofit. The control wall was unreinforced. The two retrofits include the application of 2.5 in (63.5 mm) GFRP laminate strips to the surface of the wall along the head joints and #2 GFRP NSM rods within the head joints. On the four walls that were strengthened, the FRP was anchored to the boundary members using the anchorage techniques described later in Section 4.3.

After Series I walls were tested, the test program for Series II was developed. A shear deficiency was not noticed when the wall was subjected to a static load, and therefore was not included in Series II. The first two walls of Series II serve as an additional control. An unreinforced wall was tested in the first series to serve as a control. The two controls in this series were strengthened, but do not make use of the anchorage techniques. This allowed for a direct measure of the increase in capacity associated with the use of anchorage. The walls in Series I were all constructed using a stacked bond pattern. Since many facilities are constructed using a running, or staggered, bond, it was necessary to study the effects of bond pattern. This was done by constructing two of the walls using a running bond. Both FRP retrofit techniques with

anchorage were tested using this bond pattern. Series II concluded by studying the effects of the reinforcement ratio, or the width of the laminate strip. The final two walls made use of laminate strips that were 4.5 in (114.3 mm) and 6.5 in (165.1 mm) wide to see how the capacity of the walls changes as you increase the amount of reinforcement on the walls. This change is only possible when using the laminates. The amount of reinforcement in the case of NSM bars cannot be increased without cutting additional grooves in the blocks due to the size limitations of the mortar joints.

The research program concludes with Phase II. This was the field blast testing of two walls. Under static loading, the laminates performed better than the NSM rods, so they were selected for use in this phase to evaluate their performance under dynamic loading. One wall made use of 2.5 in (63.5 mm) laminates unanchored, while the other wall had the same reinforcement, but the FRP was anchored to the boundary members and the shear retrofit is included.

This experimental program investigated the development of continuity between the FRP and the boundary members. Several other variables were also examined, including shear retrofit, the effects of bond pattern, and the effects of the width of the laminate strips. The test program is summarized in Table 4.1.

4.3. CONSTRUCTION OF WALLS

Before the URM walls could be constructed, reinforced concrete (RC) boundary members were constructed. Six walls will be constructed at a time, so twelve boundary members were needed. Standard wood formwork was constructed as illustrated in Figure 4.2 was used to cast six beams per pour. The concrete boundaries were one foot square

Table 4.1. Experimental Test Matrix

Walls			Retrofit Scheme						
			FRP Sheets	Sheet Width	NSM FRP Rods	Shear Retrofit	Anchorage	Stacked Bond	Running Bond
Phase I	Series I	#1					√		
		#2				√		√	
		#3	√	2.5"			√	√	
		#4	√	2.5"		√	√	√	
		#5			√		√	√	
		#6			√	√	√	√	
	Series II	#7	√	2.5"				√	
		#8			√			√	
		#9			√		√		√
		#10	√	2.5"			√		√
		#11	√	4.5"			√	√	
		#12	√	6.5"			√	√	
Phase II	#1	√	2.5"				√		
	#2	√	2.5"		√	√	√		

Conversion: 1 in = 25.4 mm Key: √ - includes detail



Figure 4.2. Formwork for Boundary Elements

beams, reinforced with three longitudinal #3 steel rebar top and bottom, allowing the beams to have the same strength in both directions. #3 stirrups spaced at 14 in (355.6 mm) on center were used for shear reinforcement. Two steel tube inserts were also cast within the beams to allow for easier movement and they have an integral function in the test setup as will be shown later in this section. The beam detail, completed cages and forms are illustrated in Figure 4.3. The concrete was poured using ready mix concrete from Breckenridge Ready Mix in Rolla, Missouri as illustrated in Figure 4.4 and allowed to cure in the form for 7 days. The first set of beams was removed and the forms were reassembled and the second set of six beams was cast in the same manner.

The walls used in this research program were constructed on top of one of the boundary elements. To remove errors related to the construction of the masonry walls, experienced masons from Rolla Technical Institute in Rolla, Missouri constructed the walls. The process of wall construction is illustrated in Figure 4.5. After the completion of the wall construction, the walls were allowed to cure for 14 days. After this curing

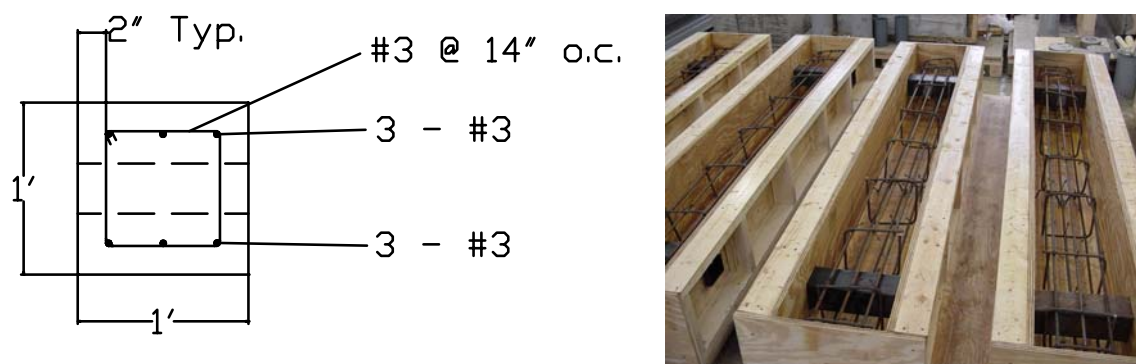
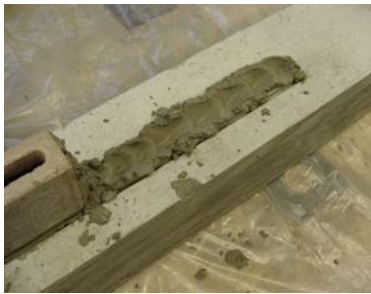


Figure 4.3. Beam Detail, Steel Cages, and Forms



Figure 4.4. Pouring Concrete



(a) Bottom Bed Joint



(b) First Course



(c) Bed Joint



(d) Second Course



(e) Completed Wall



(f) Completed Walls

Figure 4.5. Wall Construction

period the top boundary elements were placed and centered on the walls. This was done by first applying a layer of mortar to the top course and lowering the beam into place using a 20 ton (18144 kg) overhead crane in the SERL. The boundary element was supported by a steel frame system and wood members as illustrated in Figure 4.6 until the mortar had set and reached adequate strength. After the top was set, the wall was ready to be strengthened. The strengthening methods described in Section 3.2 were followed for the application of NSM GFRP rods and GFRP laminates.



Figure 4.6. Supporting Frame

As mentioned in Section 4.2, a shear retrofit was used in half of the walls in Series I. The retrofit used in this program was the grouting of the two courses of blocks in contact with the boundary members. Grouting of the bottom course is shown in Figure 4.7. To hold grout in the top course, foam was injected into the course below the top one



Figure 4.7. Grouted Bottom Course

as shown in Figure 4.8. This allowed for the insertion of grout in the top course only (Figure 4.9). In previous blast tests, shear problems occurred in the top and bottom course under blast loading. As a result, this study examined grouting the boundary



Figure 4.8. Injected Foam

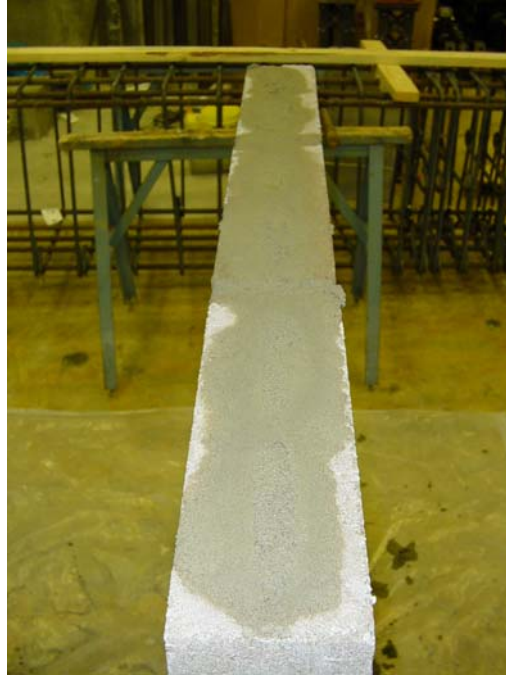


Figure 4.9. Grouted Top Course

courses rather than grouting the entire wall. This retrofit method can easily be applied to an existing wall by drilling holes into the core of the concrete blocks. Flowable grout can be injected into the bottom course. Expandable foam can be injected into the course below the top and finally, grout can be injected into the top course completing the shear retrofit as illustrated in the schematic shown in Figure 4.10.

The two retrofit techniques require some preliminary work to the boundary members prior to the wall's construction when the anchorage systems are used. For the case of NSM rods, the GFRP rebar was anchored approximately 3 in (76.2mm) deep into the concrete boundary member as shown in Figure 4.11. This was accomplished by drilling holes in the beams to line up with the location of the wall's head joints once the wall was constructed. Figure 4.12 shows a beam with the pre-drilled holes. The face of

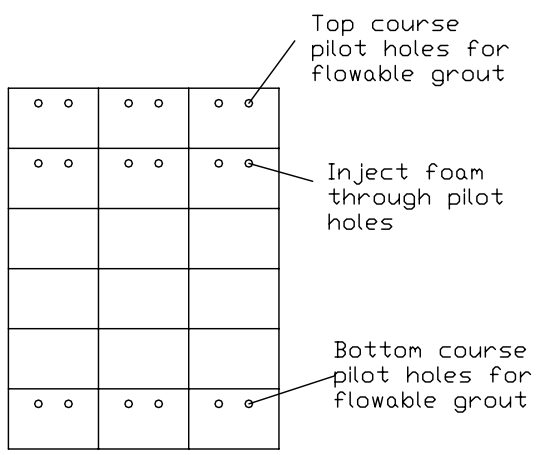


Figure 4.10. Field Application Schematic

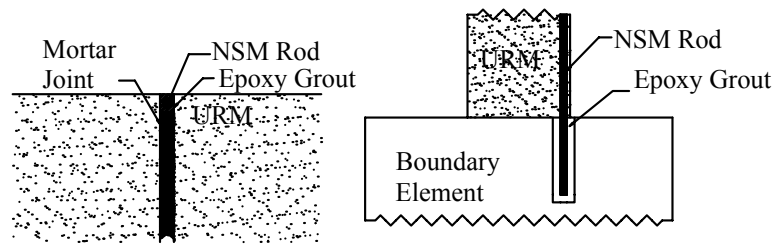


Figure 4.11. NSM Rod Anchorage



Figure 4.12. Predrilled Holes

the wall should be flush with the front edge of the hole to allow the glass bar to be installed flush with the face of the wall. After the wall was constructed on the beam, the head joints were raked out to a depth of about a half inch as shown in Figure 4.13. Figure



Figure 4.13. Raked Head Joint

4.14 shows the raked joint in line with the hole in the boundary member. If this were an actual retrofit of an existing wall, the vertical mortar joints could be ground out using a masonry grinder. The holes in the concrete could be drilled following the grinding of the joints. Holes were also pre-drilled in the top beam and were aligned as it was set in place. After the top beam was set the FRP could be applied to the wall. The GFRP bar was cut so that it could be anchored 3 in (76.2 mm) top and bottom into the concrete. The installation method described in Section 3.2 was followed. To anchor the bar, the epoxy paste was simply injected into the holes before the bar was inserted into the wall. The

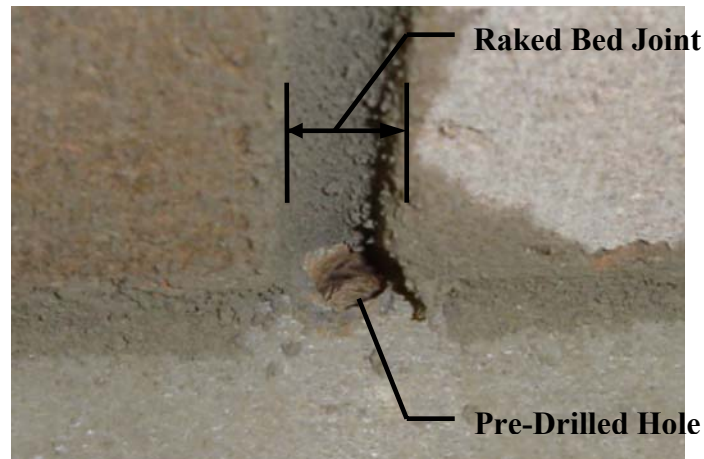


Figure 4.14. Raked Joint and Predrilled Hole

bars were flexible enough to allow them to bend to fit into the anchorage holes. Figure 4.15 shows the NSM rod set and anchored to the boundary member.

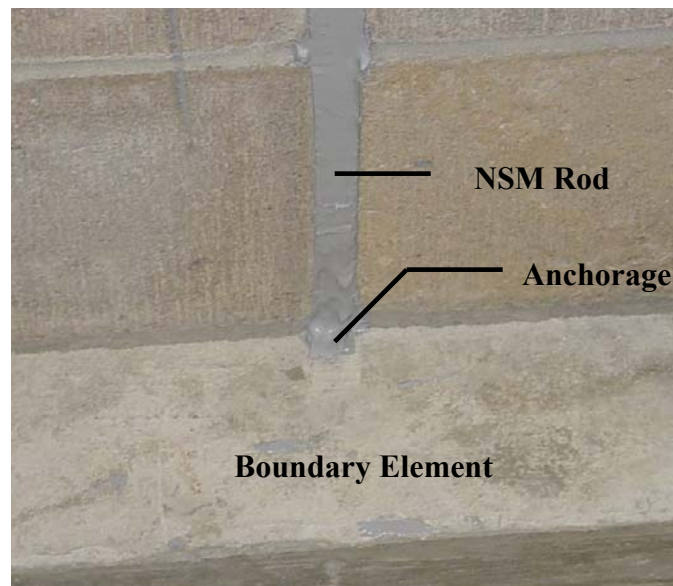


Figure 4.15. Anchored NSM Rod

The GFRP laminates were anchored in a slightly different manner. #2 GFRP rebar was also needed for this anchorage technique. This method involved the anchoring of the laminate in a groove in the concrete boundary. This was accomplished by allowing the laminate strip to wrap into the groove. A GFRP bar was epoxied into the groove to hold the strip in place. This is illustrated in Figure 4.16. First, a 0.5 in (12.7 mm) by 0.5 in (12.7 mm) groove was cut into the boundary member the length of the wall (Figure 4.17). The wall was then constructed with the face of the wall flush with the back

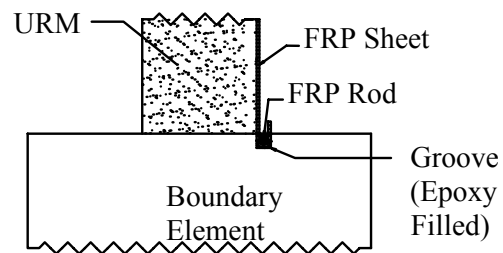


Figure 4.16. Laminates Anchorage

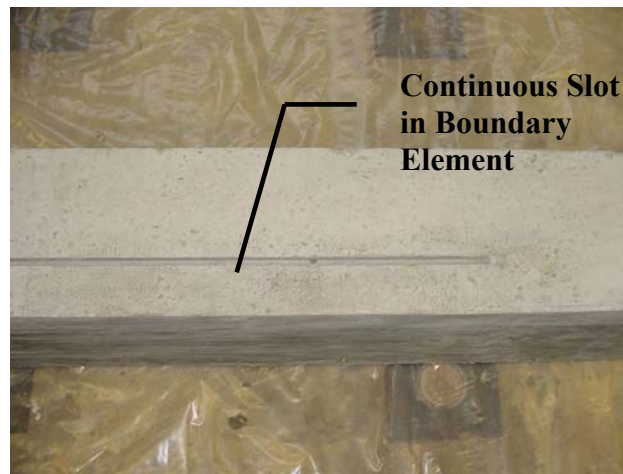


Figure 4.17. Groove in Beam

side of the groove shown in Figure 4.18. After the top beam was placed on the wall, also with a groove in it, the FRP was applied to the wall as previously described (See Section 3.2). The laminate strips were about 8 in (203.2 mm) longer than the height of the wall to have enough material to work with in the anchorage regions. Once the FRP was applied to the wall, the anchorage could begin to be installed. The sheet was wrapped into the groove as shown in Figure 4.19. The groove was filled with paste and a #2 GFRP bar was inserted into the groove as shown in Figures 4.20 and 4.21, respectively. Figure 4.22 shows the finished laminate anchorage system.



Figure 4.18. Groove with Wall Constructed



Figure 4.19. Sheet Wrapped in Groove



Figure 4.20. Groove Filled with Paste



Figure 4.21. #2 GFRP Bar Inserted into Groove

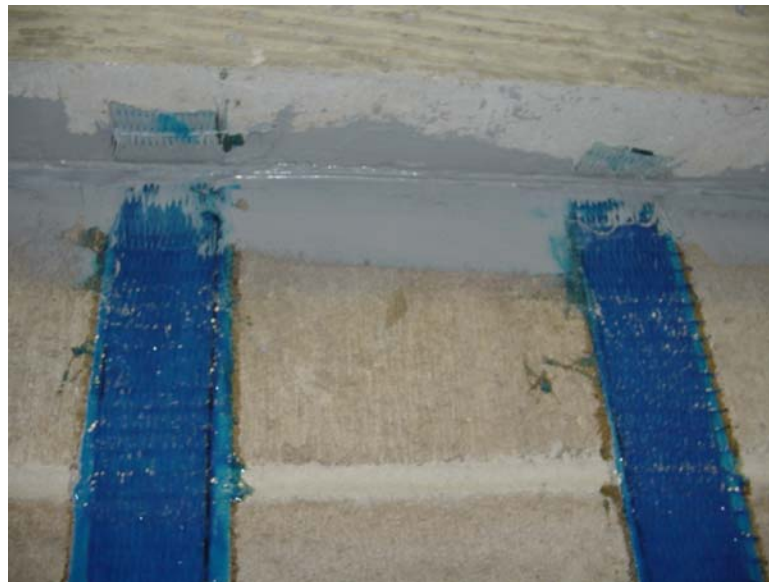


Figure 4.22. Completed GFRP Laminate Anchorage System

Part of the data collected during testing was the strain in the FRP. Prior to the insertion of the GFRP rods into the walls, strain gages were attached according to the manufacturer's recommendations at various locations. A small flat spot must be made by sanding the rods to provide a smooth surface to attach the gage. To install strain gages on the laminates, the laminates must first be installed. After the saturant has cured, it was sanded down in the location where the gage is to be applied. This is so the gage is applied directly to the fibers, not to the saturant. With the walls constructed, the anchorage details installed, and strain gages attached, the walls are ready to be tested.

4.4. TEST SETUP AND TESTING PROCEDURES – LAB

The tests for the static phase of this research were performed in the high-bay structures lab (SERL) in Butler-Carlton Civil Engineering Hall at UMR. The walls were constructed outside of the test area and moved into testing position using the lab's 20 ton (18144 kg) bridge crane.

Structural steel tubing was inserted into the inserts that were cast into the concrete boundary members. These tubes had holes drilled in them to allow dywidag bars to pass through them. These bars were used to anchor the wall to the strong floor to prevent boundary rotation and/or translation. The lab's strong wall was used as a reaction structure. To fill the space between the test wall and the strong wall, CMU blocks were stacked up to fill all of the space, leaving just enough room to insert the air bag loading mechanism. Two air hoses run to the test setup. One of the lines is the actual air inflow line. An air compressor was used to fill the bag. The pressure in the bag could be regulated from a safe distance using an in line pressure regulating valve. The other line

was connected to the fill line at the bag's fill port. A pressure gage was connected to the other end of this line to allow the pressure in the bag to be measured. A chain was anchored to the strong wall and placed around the top boundary element in an attempt to limit any translation of the top boundary element. The test setup is illustrated in Figure 4.23.

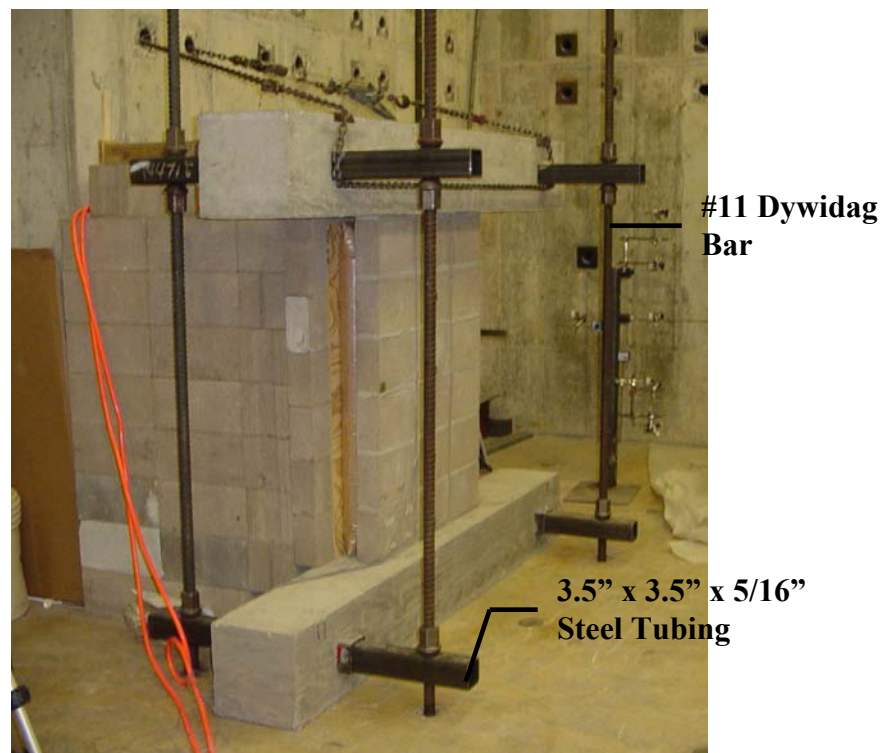


Figure 4.23. Test Setup

The strain in the FRP was measured at six locations during leading using the strain gages that were applied as previously discussed. The gages were located in approximately the same location on each wall. The light spots on the FRP in Figure 4.24



Figure 4.24. Strain Gage Locations

are the locations where the gages were applied. Strain readings were taken using individual strain indicators for each gage. To measure deflections, two methods were used. Dial gages were used to accurately measure deflections during the initial loading stages of the test. Six dial gages were used to measure deflection. Five gages were placed in the middle of the wall vertically, two at the ends, one at midspan, and two at the quarter points. To ensure the load was distributed uniformly in the horizontal direction, and additional deflection reading was taken near the walls edge at midspan. The dial gage setup is shown in Figure 4.25. During testing, safety became an issue where the physical reading of deformation was no longer safe. At this point, the gages were removed and a digital high power video camera is used to record precise ruler measurements. A precise ruler was attached to the CMU fill material as shown in Figure



Figure 4.25. Dial Gage Setup

4.26. The ruler was accurate to 0.0625 in (1.59 mm). A video camera records as the wall is tested, and the wall's movement relative to the precise ruler can be observed and recorded.

The testing procedure was rather simple. The pressure in the air bag was incrementally increased, causing the load on the wall to increase. At each pressure increment, the pressure in the bag was recorded. The strain at each of the strain gage location was taken from the strain indicators. Finally, each of the six dial gage readings were read and recorded. The pressure was increased in 0.1 psi (0.69 kPa) increments for Walls #1-#3. For Walls #4 - #12, the increment was 0.2 psi (1.38 kPa). After testing the first three walls the pressure gage was changed to allow for an increased maximum pressure. This was done as the strengthened walls were expected to have greater capacity. This process of increasing the load and taking strain and dial gage readings continued until it was determined it was no longer safe to be in close proximity to the

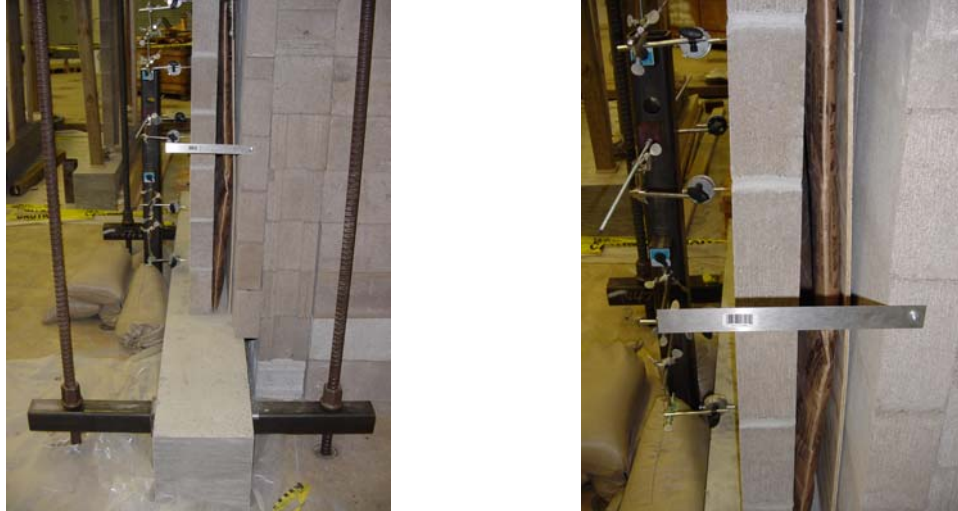


Figure 4.26. Precise Ruler for Deflection Measurement

wall. At this point, the dial gages were removed and strain gages unhooked from the indicators. From this point until failure, deflection readings were recorded by the video camera as the pressure readings were called out at each load increment. Load was continued to be applied until the wall reached failure. The results from these tests are presented in Section 5.

4.5. TEST SETUP AND TESTING PROCEDURES – FIELD

The test setup for this portion of the research program was similar to the setup used in the static testing performed in the structural engineering research laboratory. These tests were conducted on a firing range at the United States' Ft. Leonard Wood Army Base in St. Robert, Missouri. This same range was used for previous blast testing by El-Domiaty et al. Concrete pads were constructed on site to serve as the foundation for test walls. The pads were constructed in series of two. A steel reaction frame was

fabricated and delivered to the site to rest on the two pads and provide support for the top boundary members. It should be noted that this frame was originally constructed for 88 in (2235.2 mm) tall walls, so additional support construction was required for this test. All of the details for the foundation system and reaction frame may be referenced in a report prepared by El-Domiaty et al. (2002). To minimize the need for a crane on site, a wood frame was constructed to support the top beam so the infill wall could be constructed between the two boundaries. Figure 4.27 shows the test setup with the steel frame, wood frames, and boundary members in place prior to construction of the walls. With the preliminary setup completed the walls could be constructed between the boundaries.

Two walls were tested in Phase II. The walls used in this phase of the research program are the same as Walls #4 and #7 used in Phase I. One of them was strengthened



Figure 4.27. Frame and Boundary Setup

with 2.5 in (63.5 mm) wide strips not anchored to the boundaries. The other makes use of the same reinforcement, but the FRP will be anchored to the boundaries and will also include the shear retrofit. The completed test setup is shown in Figure 4.28.



Figure 4.28. Phase II Test Setup

To test the walls, a series of explosive charges was used to evaluate the wall's performance after each charge. The explosive used in this test was Pentolite dynamite, which is a 50/50 mixture of TNT and C4. The charge weight was increased for each blast in the series until the range's charge limit is reached. The charge was suspended from a rope at the mid-height of the wall at the given standoff distance as illustrated in Figure 4.29. Table 4.2 summarizes the blast events undertaken and uses Equation 2.9 to predict

the pressures that were developed on the front face of the wall. The results from this phase of the research are presented in Section 5.



Figure 4.29. Suspension of Charge

Table 4.2. Summary of Blast Events

Wall	Charge Weight (lb)	Standoff Distance (ft)	Face Pressure (psi)
Wall #1	2	6	151
	4	6	302
Wall #2	3	6	227
	4	6	302
	5	6	378

Conversions: 1 ft = 12 in = 25.4 mm, 1 psi = 6.895 kPa, 1 lb = 0.45 kg

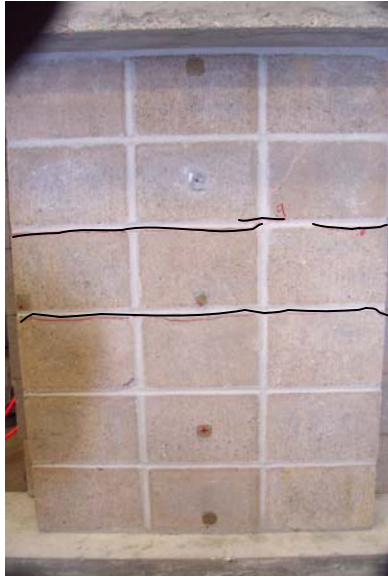
5. RESULTS AND DISCUSSION

5.1. LABORATORY RESULTS

This section presents the results of the static load testing phase of this research program. Of the twelve walls tested in this phase of the research program, none exhibited a shear problem or failure near the supports. As a result, the shear retrofit that was implemented could not be evaluated in the static test phase. When arching action is present, two possible failures can occur. The first is crushing of the masonry block and the second is the snapping through of the two rotating panels before crushing occurs. None of the walls showed signs of CMU crushing. The out-of-plane performance, development of arching action, and a description of the failure mode are provided for each wall. Plots of deflected shape, pressure versus midspan deflection, and pressure versus strain are provided for each wall in Appendix A.

5.1.1. Wall #1. Wall #1 was the first of the two unreinforced control walls. As testing began, an initial crack formed above the fourth course at 0.6 psi (4.1 kPa). Rotation, or the development of arching action, could be observed at the bottom of the wall. At 3.0 psi (20.7 kPa), a crack at the midspan joint occurred as shown in Figure 5.1a. After the crack occurred at midspan, a distinct development of arching action was observed just prior to failure as seen in Figure 5.1b. Wall #1 failed at a pressure of 5.3 psi (36.5 kPa) with a deflection at failure of 1.3 in (33 mm). The failure is shown in Figure 5.1c.

5.1.2. Wall #2. Wall #2 was an unreinforced control with a shear retrofit. This wall performed much the same as Wall #1. Initial cracking was at the fourth course and occurred at 3.1psi (21.4 kPa). Midspan cracking occurred at 4.0 psi (27.6 kPa) and



(a) Cracking



(b) Arching Action



(c) Failure

Figure 5.1. Wall #1 Failure

development of arching action occurred as shown in Figures 5.2a and 5.2b respectively. Loading continued until failure (Figure 5.2c) with an ultimate load of 6.6 psi (45.5 kPa) and a deflection at failure of 0.74 in (18.8 mm).



(a) Cracking



(b) Arching Action



(c) Failure

Figure 5.2. Wall #2 Failure

5.1.3. Wall #3. Wall #3 was reinforced with 2.5 in (63.5 mm) wide sheets along the head joints. The sheets were anchored to the boundary members in this case. Initial cracking occurred at midspan at 3.1 psi (21.4 kPa), immediately followed by a crack above the fourth course at 3.2 psi (22.1 kPa). At 4.1 psi (28.3 kPa), a crack formed at the bottom course. Propagating cracks began to form at the intersection of the midspan crack and the GFRP sheet as shown in Figure 5.3a. This was followed by the cracking of the

block and additional propagation of cracks at midspan as well as above the fourth and fifth course (Figures 5.3b and 5.3c). Distinct arching began to occur and a form of delamination was observed (Figure 5.3d). The wall failed at 12 psi (82.7 kPa) with a deflection at failure of 1.5 in (38.1 mm). As the wall failed, pullout of the top anchorage occurred initially followed by the shearing of the sheets at the connection to the bottom boundary member. The rebar anchoring the sheets to the top member was broken near the location where the sheet was wrapped around it (Figure 5.3e). The anchorage bar also pulled out of the top groove within the boundary element very clean, indicating that the bond between the rod and the paste may not have been good. The failure of the FRP can be classified as a delamination failure. However, there was no separation of the laminate from the wall. Concrete remained attached to the sheet after failure. The tensile strength of the concrete is reached before the bond breaks (Figure 5.3f).

5.1.4. Wall #4. Wall #4 was also reinforced with 2.5 in (63.5 mm) GFRP sheets. This wall had an ultimate capacity of 11.4 psi (78.6 kPa) and a maximum deflection of 1.1 in (27.9 mm). Midspan cracks formed at 3.4 psi (23.4 kPa) and a crack formed above the fourth course at 3.8 psi (26.2 kPa). This wall also displayed the propagation of cracks as did the previous wall (Figure 5.4a). Delamination was also present just prior to failure. Initially, the FRP ruptured at midspan, followed by shearing of the sheets at the bottom. There was a partial pullout at the top. One of the sheets pulled off the embedded rebar, while part of the other one stayed in tact (Figure 5.4b). The top bar in this case also appeared to be pulling out fairly clean.



(a) Propagation of Cracks



(b) Crack Through Block



(c) Cracking



(d) Delamination



(e) Pullout



(f) Masonry Attached to Laminate

Figure 5.3. Wall #3 Failure



(a) Cracking

(b) Pullout

Figure 5.4. Wall #4 Failure

5.1.5. Wall #5. This wall was reinforced with two #2 GFRP bars along the head joints. The bars were anchored approximately three inches into the concrete boundary members. The failure occurred with the shearing of the FRP at three of the four connections. The fourth remained epoxied into the boundary member. Cracking began in this wall at 3.8 psi (26.2 kPa) with a midspan crack. Additional cracking continued with a crack above the fourth course at 4.4 psi (30.3 kPa). Several cracks formed through the blocks as shown in Figure 5.5a. Failure occurred at 10.2 psi (70.3 kPa) and a deflection of 1.2 in (30.5 mm) (Figure 5.5b).

5.1.6. Wall #6. The cracking of Wall #6 began at 2.6 psi (17.9 kPa) with a crack above the fourth course. This was followed by a midspan crack at 3.4 psi (23.4 kPa). During testing, the chain restraining translation of the top boundary broke. As a result, the pressure was decreased to a safe working level and the chain was replaced. Loading was then continued until failure was reached at a deflection of 1.1 in (27.9 mm) and a



(a) Cracking

(b) Failure

Figure 5.5. Wall #5 Failure

load of 11 psi (75.8 kPa). Failure occurred at midspan with the rupture of one of the FRP bars. The other bar pulled out of the bottom boundary, but remained attached at the top.

5.1.7. Wall #7. This was the first wall tested as part of Series II. This wall was reinforced with 2.5 in (63.5 mm) GFRP sheets that were not anchored to the concrete boundaries. An initial midspan crack occurred at 2.0 psi (13.8 kPa). At 2.4 psi (16.5 kPa), a crack formed above the fourth course. As was the case with the previous wall reinforced with sheets, propagating cracks began to form at midspan (Figure 5.6a). Cracks illustrating the arching action can be seen in Figure 5.6b. Additional cracks formed through the blocks, as well as diagonal crack through the blocks visible from the side of the wall (Figure 5.6c). Delamination of the FRP occurred just prior to failure. A pressure of 9.6 psi (66.2 kPa) was achieved at a displacement of 1.8 in (45.7 mm). This wall test demonstrated the importance of anchoring the bonded laminates.

5.1.8. Wall #8. Wall #8 was reinforced with two unanchored #2 GFRP rebar. Initial cracks formed at midspan and above the fourth course. Propagation of cracks



(a) Cracking



(b) Arching Action



(c) Crack on Side of Block

Figure 5.6. Wall #7 Failure

(Figure 5.7a) continued with a failure (Figure 5.7b) at 4.8 psi (33.1 kPa), a load similar to the unreinforced condition. The deflection at failure was 0.96 in (24.4 kPa).

5.1.9. Wall #9. This wall was reinforced with NSM rods and made use of a running bond pattern, so the rods actually pass through some of the blocks. Cracking began above the fourth course at 2.2 psi (15.2 kPa) and at midspan at 3.0 psi (20.7 kPa). Extensive crack propagation was present, as were cracks through the blocks (Figure



(a) Cracking

(b) Failure

Figure 5.7. Wall #8 Failure

5.8a). Arching action was also clearly defined (Figures 5.8b and c). 9.4 psi (64.8 kPa) was the failure load that occurred at 1.3 in (33.0 mm) of lateral displacement. The GFRP rods sheared off at the top, and one pulled out of the boundary at the bottom (Figures 5.8d and e).

5.1.10. Wall #10. Wall #10 was reinforced with 2.5 in (63.5 mm) wide laminate strips anchored to the boundary. This wall was constructed using the running bond pattern. Initial cracking occurred above the fourth and fifth courses and at midspan at 1.8 psi (12.4 kPa). Propagating cracks began to occur at midspan and above the fourth course. Distinct arching action could be observed (Figures 5.9a and b). The propagation of cracks continued with additional cracking through the blocks. Failure as shown in Figure 5.9c occurred at a pressure of 11.0 psi (75.8 kPa) and a displacement of 1.7 in (43.2 mm). Delamination was observed as were diagonal cracks through the 4 in (101.6 mm) dimension of the blocks (Figure 5.9d). Pullout from the top beam occurred (Figure

5.9e), but a portion of the rod remained in the beam. The FRP was sheared at the bottom boundary (Figure 5.9f).



(a) Cracking



(b) Arching Action



(c) Arching Action



(d) Sheared Connection



(e) Pullout

Figure 5.8. Wall #9 Failure



(a) Arching Action



(b) Arching Action



(c) Failure



(d) Crack on Side of Block



(e) Pullout



(f) Sheared Connection

Figure 5.9. Wall #10 Failure

5.1.11. Wall #11. Wall #11 was reinforced with 4.5 in (111.8 mm) anchored FRP Sheets. This wall failed at a deflection of 1.9 in (48.3 mm) and a load of 12.6 psi (86.9 kPa). Cracking began at 2.0 psi (13.8 kPa) above the fourth course, followed by a crack at midspan at 2.8 psi (19.3 kPa). At 3.6 psi (24.8 kPa) there was a crack above the fifth course. Arching action and propagation of cracks were observed. There was also a shear crack through the block. Additional propagating cracks and cracks through the blocks were observed. Extensive cracking (Figure 5.10a) occurred prior to the delamination failure at 12.6 psi (86.9 kPa). At the failure deflection of 1.9 in (48.3 mm), the FRP sheets pulled off of the bar anchoring them to the top boundary (Figure 5.10b) and sheared off at the bottom. The integrity of the wall system was generally intact after failure (Figure 5.10c).

5.1.12. Wall #12. Wall #12 had the highest reinforcement ratio of all of the walls tested in Phase I. This wall was reinforced with 6.5 in (165.1 mm) wide sheets anchored to the boundaries. At 2.6 psi (17.9 kPa), cracks formed at midspan and above the fourth course. This was followed by additional cracking at 4.6 and 4.8 psi (31.7 and 33.1 kPa) above the fifth and second course respectively. Initial failure was the pullout of the FRP sheets from the bottom beam followed by pullout from the top (Figure 5.11a). This failure occurred at 15.2 psi (104.8 kPa) and a deflection of 1.9 in (48.3 mm). Arching and propagation cracks and cracks through the blocks were present (Figure 5.11b). The laminates held the system intact after failure (Figure 5.11a).



(a) Cracking



(b) Pullout



(c) Wall Held Together

Figure 5.10. Wall #11 Failure



(a) Pullout



(b) Cracking

Figure 5.11. Wall #12 Failure

5.2. FIELD RESULTS

This section presents the results of Phase II, the field blast testing phase of this research program. Four damage levels have been established to categorize the damage caused by a blast load to test walls. These damage levels are summarized in Table 5.1. Table 5.2 summarizes the blast loadings undertaken by the walls in this phase, as well as the level of damage the wall sustained under each loading.

5.2.1. Wall #1. Wall #1 was strengthened with 2.5 in (63.5 mm) GFRP laminates. No anchorage detail was provided for this wall. The wall survived the first blast event of 2 lb (0.9 kg) with minimal cracking sustaining light damage. The second blast event made use of 4 lb (1.8 kg) of pentolite explosive and caused a failure as illustrated in Figure 5.12. Extensive cracking occurred in all of the mortar joints with a sliding failure of the mortar joint between the top course of blocks and the top boundary

Table 5.1. Levels of Damage to Tested Walls (El-Domiaty et al. 2002)

Level	Damage Level	Damage Description	Performance Description
I	Failure	Wall falls out of test frame.	Wall crumbles and scattered debris.
II	Heavy Damage	Damage that definitely affects load capacity of wall. Wall will not survive same blast load.	Visible wide-open cracks or significant shear cracks, and damage to FRP retrofit. Small debris close to the wall
III	Light Damage	Damage that does not affect load capacity but additional damage will be observed under same blast load.	Hairline to wider cracks at mortar joints or hairline shear cracks.
IV	No Damage	No damage affecting load capacity of wall.	Hairline cracks in mortar joints.

Table 5.2. Summary of Blast Events and Levels of Failure

Wall	Charge Weight (lb)	Standoff Distance (ft)	Level of Damage
Wall #1	2	6	Light Damage
	4	6	Failure
Wall #2	3	6	Light Damage
	4	6	Heavy Damage
	5	6	Failure

Conversions: 1 ft = 12 in =25.4 mm, 1 lb = 0.45 kg

element. Cracks formed through the blocks and a diagonal crack formed on the side of a mid-height block (Figure 5.13).

5.2.2. Wall #2. Wall #2 was strengthened with 2.5 in (63.5 mm) GFRP laminates that were anchored to the boundary members. The shear retrofit was also included in the construction of this wall. This wall survived the first blast of 3 lb (1.4 kg) with light damage consisting of minimal cracking in some of the mortar joints. The following blast



(a) Side View



(b) Sliding Failure at Boundary Element



(c) Front View

Figure 5.12. Wall #1 Failure



(a) Cracking Through Blocks



(b) Crack on Side of Block

Figure 5.13. Cracking

event induced heavy damage on the wall as seen in Figure 5.14. The column of blocks on the end began to rotate about the head joint where the FRP was bonding this column to the center column. Failure occurred after the 5 lb (2.3 kg) charge was set off as illustrated in Figure 5.15. Further rotation occurred with the loss of one of the blocks from the wall. The anchorage details remained intact. Propagating cracks near the midspan mortar joint indicate that the wall system was approaching the onset of delamination.

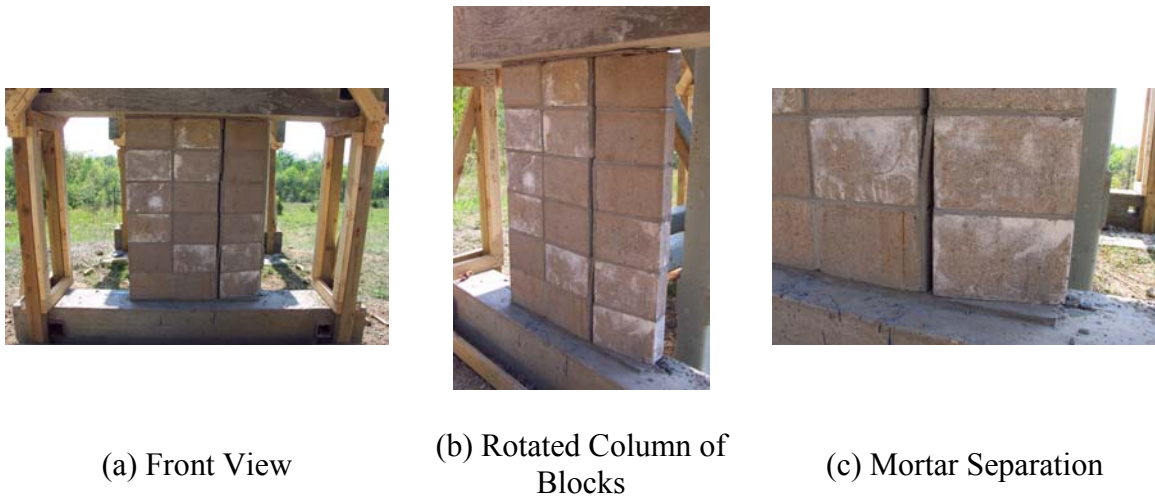


Figure 5.14. Damaged Wall

5.3. DISCUSSION

As the results indicate, strengthening the walls with FRP materials does in fact increase the wall's resistance to out-of-plane loads. Furthermore, the anchorage details allow for the development of continuity between the FRP and the concrete boundary



Figure 5.15. Wall #2 Failure

elements. This can be seen by comparing the results of Walls #7 and #8 to Walls #3 through #6 (Figure 5.16). Walls #3 through #6 investigate the condition in which the reinforcement is anchored to the boundary members. In Walls #7 and #8, the same reinforcement is used without the anchorage. For the case of the GFRP sheets, the unanchored condition provides a capacity between the unreinforced case and the anchored case. Some benefit can be obtained just by applying the sheets to the walls. When anchorage of the sheets is provided, this research suggests additional capacity is gained. This is not true in the case of the NSM rods. When the NSM rods are installed without anchoring them to the boundary, they behave in much the same way as an unreinforced wall. When anchorage is provided, continuity is developed and additional capacity is obtained.

Walls #9 and #10 examined the effects of a URM wall's bond pattern on the strength increase provided by the FRP. These two walls were constructed using a running bond, so the FRP does not follow a continuous mortar joint. The FRP was

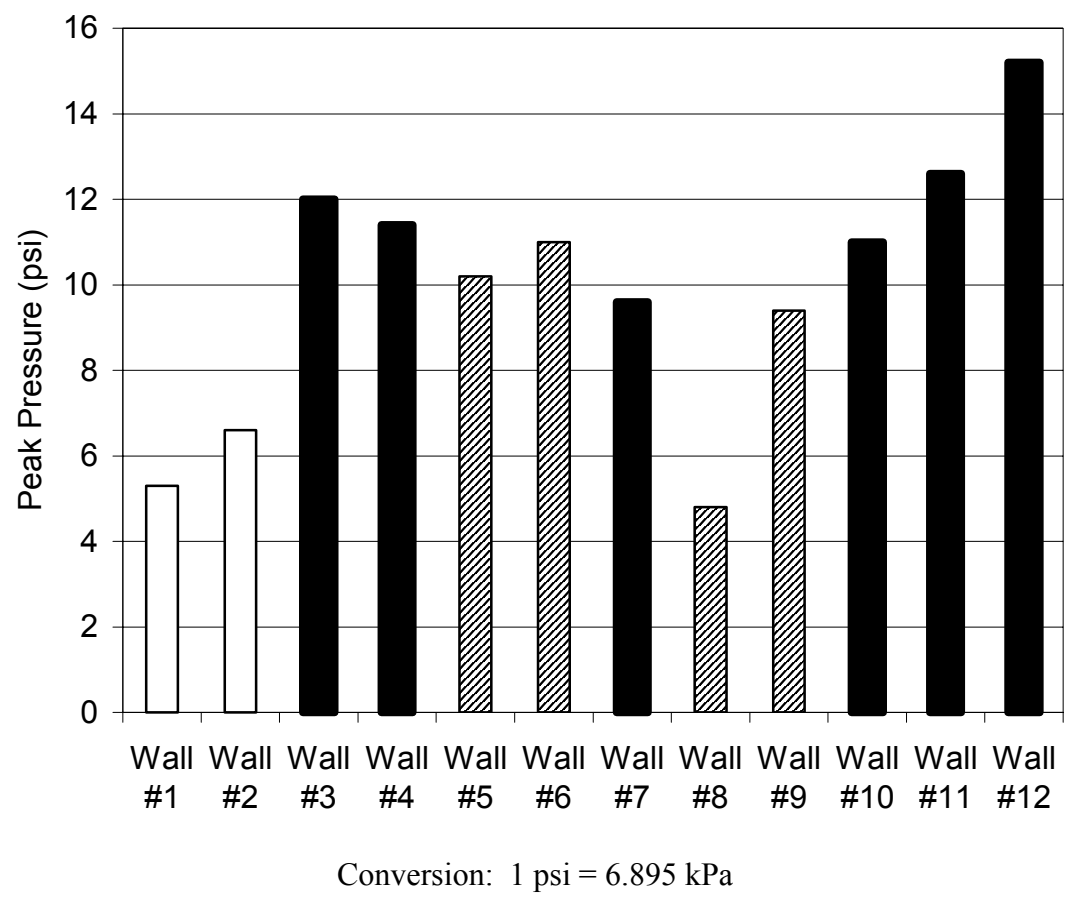
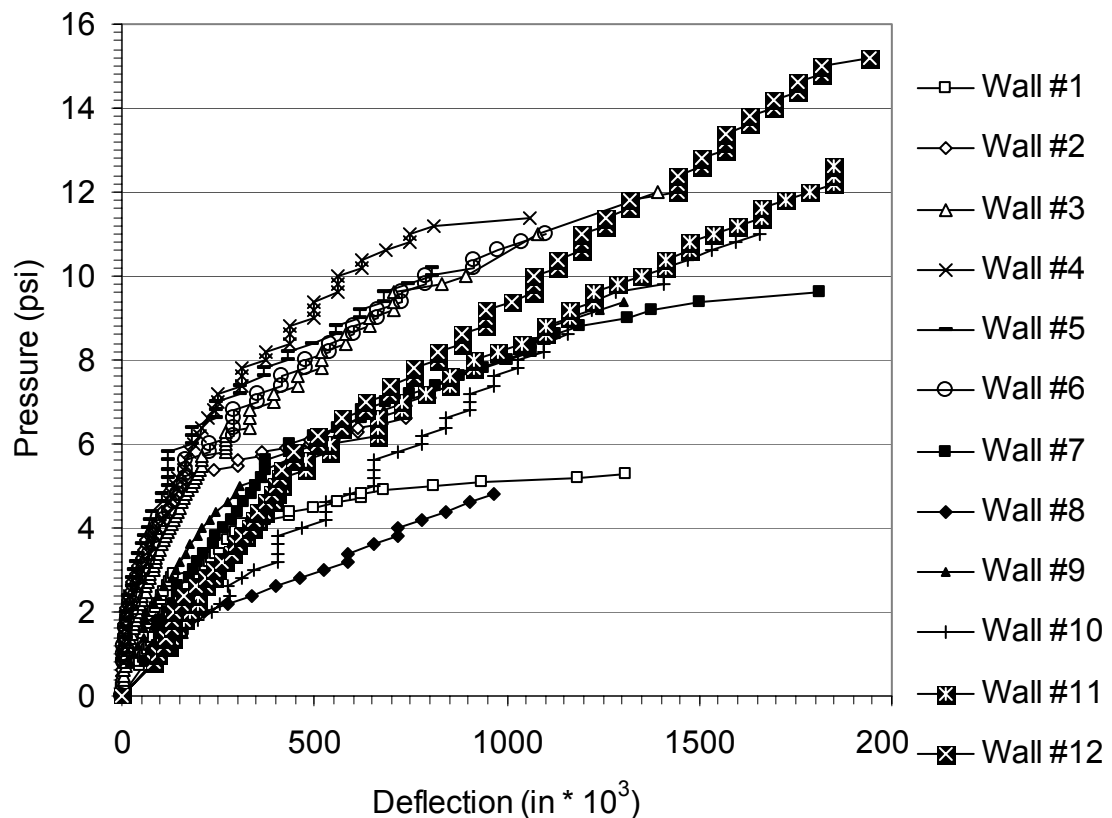


Figure 5.16. Peak Out-of-Plane Pressure Results for Phase I Test Walls at Failure

anchored to the beams for this case. The walls performed similarly to those using the stacked bond used in the rest of the test program. Though not examined in this research, bond pattern may have an effect on the case where unanchored NSM rods are used. In this case, the rods would run through the face of the blocks in every other row. This may provide an increase in strength over the case of a stacked bond where the rod is placed in a continuous joint.

Walls #11 and #12 evaluate the influence of the width of the GFRP laminates on the out-of-plane strength. It is evident that as the width increases, the failure load also increases. As a rule, an increase in the strain energy, or area under the load deflection curve, usually provides a more desirable mode of failure. The load versus deflection curves for each wall are provided in Figure 5.17. From this figure, two distinctly different initial stiffness values can be observed. The Series I walls have an increased stiffness over the walls from Series II. This is due to a variation in the compressive



Conversions: 1 psi = 6.895 kPa, 1 in = 25.4 mm

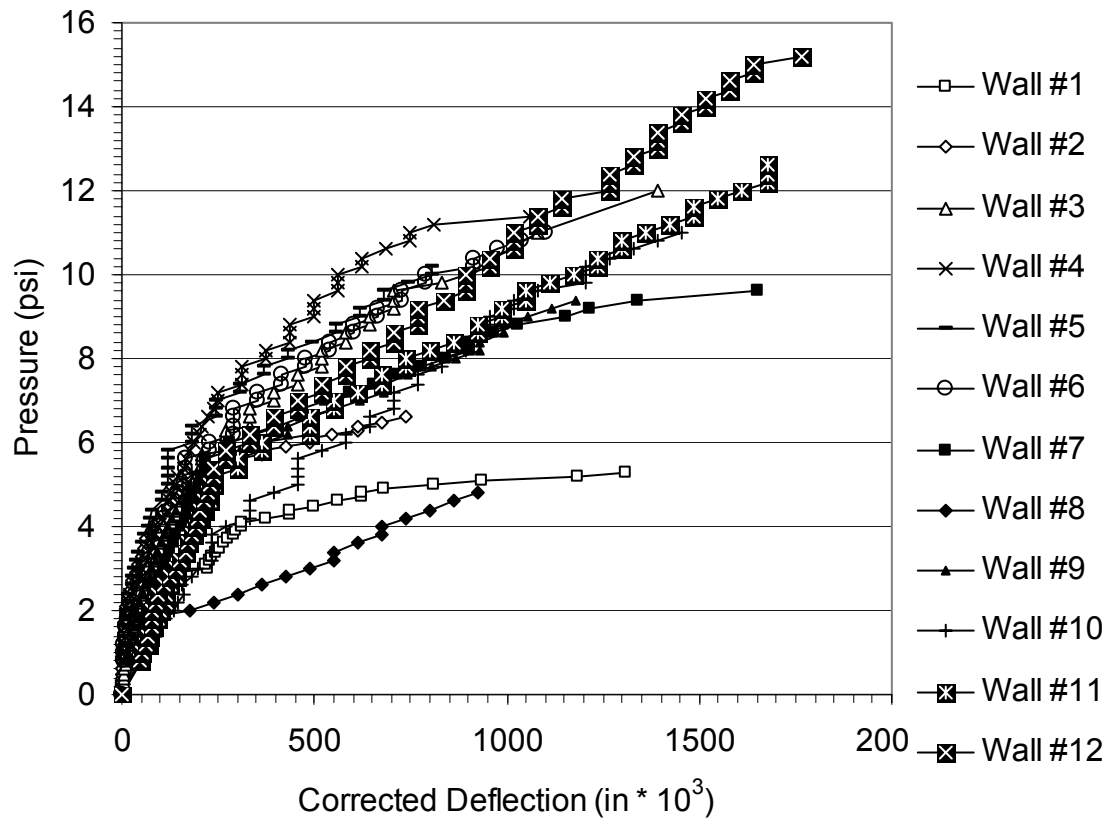
Figure 5.17. Pressure versus Displacement for Phase I Walls

strength of the mortar as reported in Table 3.4. These two series of walls were constructed at different times, and as a result had different mortar compressive strengths even though their material compositions were similar. To allow for a more accurate comparison, a correction was performed. This was done by adjusting the deflections of the elastic portion of Series II walls. According to the Masonry Standards Joint Committee (2002), the mortar's modulus of elasticity is directly proportional to its compressive strength as shown in Equation 5.1. The measured deflections from Series II

$$E_g = 500 * f'_g \quad (\text{Equation 5.1})$$

were corrected by multiplying them by the ratio of their mortar strength to that of the walls in Series I. Essentially Series II walls were normalized based on the modulus of Series I walls. The deflections beyond the linear range (elastic wall response) were simply shifted the amount of the correction at the end of the linear range since the mortar had cracked and no longer contributed in a significant fashion to the stiffness of the wall system. The corrected load versus deflection plot is illustrated in Figure 5.18.

Using the plot of pressure versus corrected deflection illustrated in Figure 5.18, the strain energy of each wall can be calculated by estimating the area under this load versus deformation curve. For this research, Wall #1 was used as a control or benchmark on which to base a strain energy ratio. The normalized strain energy as shown in Figure 5.19 is the ratio of the strain energy of a given wall to that of the control wall, Wall #1. From this figure, it is clear that the laminates provide the system with the ability to absorb more energy prior to failure. This was observed visually during the out-of-plane tests well. The walls strengthened with NSM rods failed in a brittle manner. When the laminates were used, more of the wall was held together, and you could usually tell when



Conversions: 1 psi = 6.895 kPa, 1 in = 25.4 mm

Figure 5.18. Pressure versus Corrected Displacement

the wall was approaching failure by the crack patterns. Table 5.3 summarizes the initial failure modes for each wall and categorizes the failure as brittle or ductile based on their normalized strain energy ratio.

Two different methods were used to compare the ductility of the reinforcing techniques. The first method is the deflection ductility. This is calculated by dividing the wall's ultimate deflection (u_f) by its deflection at the apparent yield point (u_y). The second method is the energy ductility. This is determined by dividing the total area under

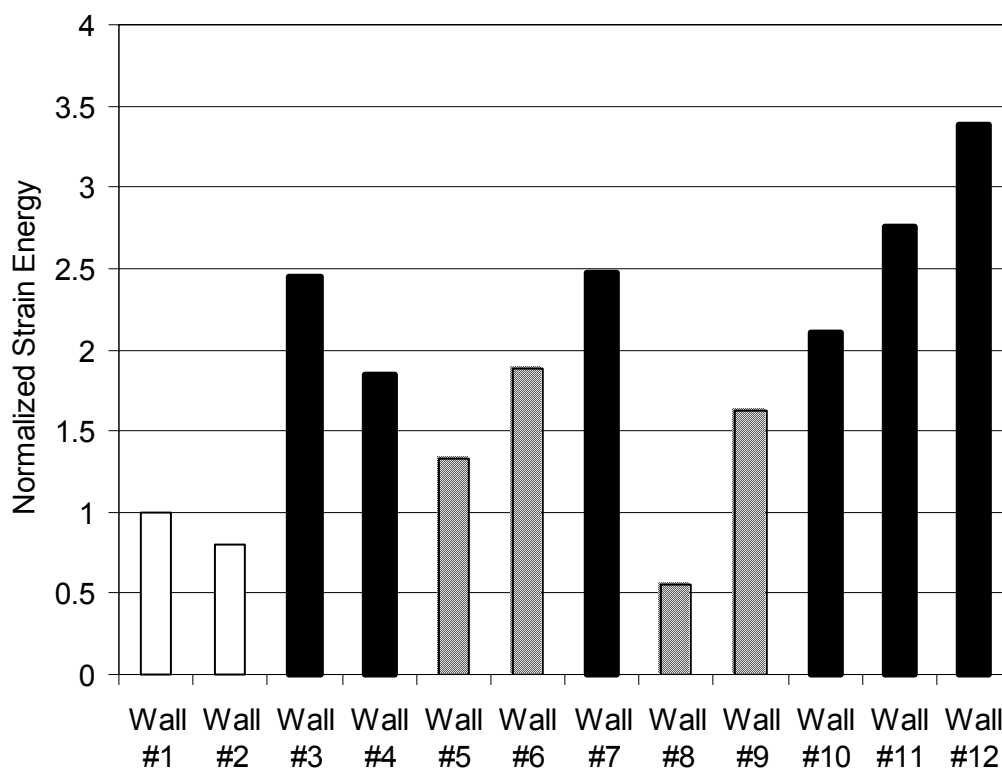


Figure 5.19. Normalized Strain Energy Ratio

Table 5.3. Summary of Failure Modes for Phase I

Wall	Initial Failure Mode	Brittle / Ductile
1	Bed Joint Failure	Brittle
2	Bed Joint Failure	Brittle
3	Delamination	Ductile
4	Delamination / FRP Rupture	Neutral
5	FRP Shear at Connections	Brittle
6	FRP Rupture	Neutral
7	Delamination	Ductile
8	Bed Joint Failure	Brittle
9	FRP Shear and Pullout at Connections	Neutral
10	Delamination	Ductile
11	Delamination	Ductile
12	Connection Pullout	Ductile

the pressure versus corrected deflection plot by the area under the linear portion of the plot. Often, energy ductility is used to characterize and discuss the ductility of composite systems. Figure 5.20 shows both the normalized deflection and energy ductility based on the control wall, as well as for the walls strengthened with 2.5 in (63.5 mm) GFRP sheets and #2 NSM GFRP rods.

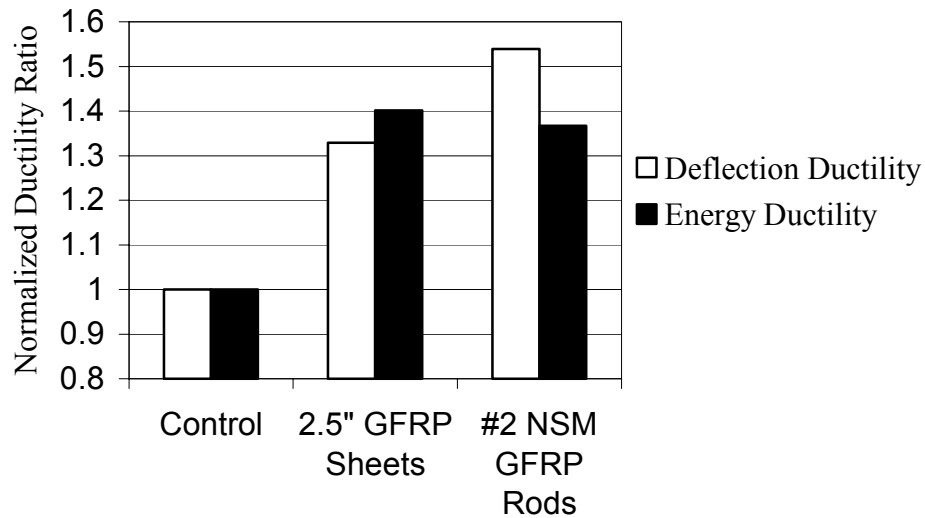


Figure 5.20. Strengthening Scheme Effects on Normalized Ductility Ratio

For comparison, the ductility has been normalized with respect to the control wall. As illustrated in the figure based on two different ductility terms, strengthening the walls with both sheets and rods provides the wall system with additional ductility. Figure 5.21 illustrates the relationship between increasing laminate strip width and ductility. In this

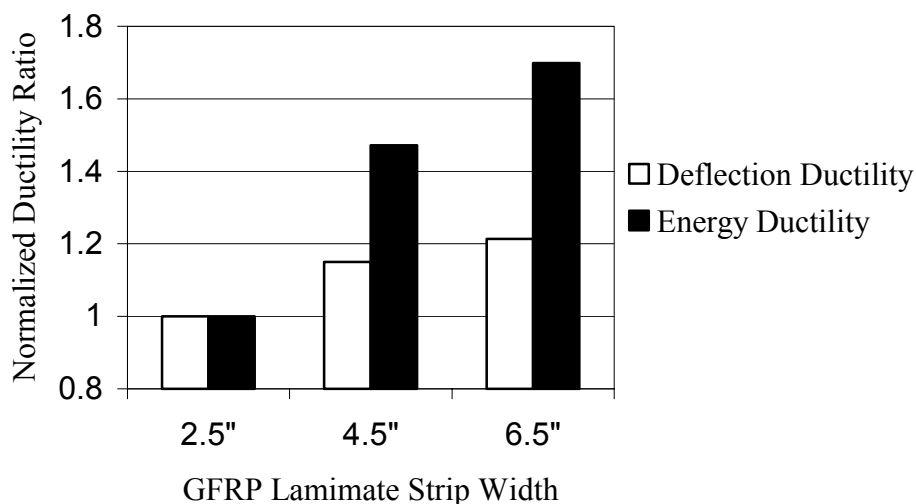


Figure 5.21. Laminate Strip Width Effects on Normalized Ductility Ratio

Figure, the ductility ratio has been normalized with respect to the wall strengthened with 2.5 in (63.5 mm) wide sheets (the lowest reinforcement ratio). Again, the ductility increases as additional strengthening is provided. In the case of the sheets, as the ductility increased, the ability of the GFRP laminates to hold the wall together also increased. As shown in the results for Walls #11 and #12, the walls were largely held in tact as the amount of reinforcement and ductility increased.

The ability of the FRP to hold the wall together upon failure is important under blast loading. People can often survive a blast, but when hit by flying objects and debris, loss of life may occur. The pressures that would cause loss of life to a human are significantly higher than those that cause catastrophic damage to a building. If the integrity of walls in a building can be maintained, there is a reduced amount of flying

debris that could potentially injure the occupants of the building. Increasing the amount of GFRP laminates on the wall was shown to improve the integrity of the wall system.

In several of the cases where the GFRP laminates were anchored to the boundaries, the GFRP rod used in the anchorage detail pulled out of the groove. Upon observation of the rod after failure, it was noted that little or no epoxy paste was still attached to the rod. This indicates that integrity of the system at higher reinforcement ratios is limited by the bond of the epoxy to the rod, and should be closely studied in future research.

To allow for the correlation of these results to those predicted by theory, an equivalent uniform load must be calculated. As the air bag inflates an area around the edges of the wall is left unloaded due to the size and shape of the air bag. To develop an expression for the equivalent uniform pressure, simple span conditions were assumed. The moment caused by loading the reduced area was determined. The required pressure to cause this same moment given a uniform load over the entire wall was then calculated. It was determined that the equivalent uniform pressure was 66.3% of the pressure recorded during testing (See Appendix B). Table 5.4 shows the equivalent uniform pressures for each wall.

The theory developed by Shapiro et. al. (1994) can be used to predict the capacity of the unreinforced wall. This theory makes use of three coefficients, R_1 , R_2 , and λ . R_1 is taken as 1.0 because there is no previous cracking. R_2 is taken as the minimum value of 0.5 because there is no framing along the sides of the wall. λ was taken as 0.0496, based on the wall's slenderness ratio. This theory predicts an out-of-plane capacity of about 5.58 psi (38.5 kPa). This value is slightly higher than the causing failure of the test

Table 5.4. Equivalent Uniform Pressures

Wall #	Experimental Pressure (psi)	Equivalent Uniform Pressure (psi)
1	5.3	3.5
2	6.6	4.4
3	12.0	8.0
4	11.4	7.6
5	10.2	6.8
6	11.0	7.3
7	9.6	6.4
8	4.8	3.2
9	9.4	6.2
10	11.0	7.3
11	12.6	8.4
12	15.2	10.1

Conversion: 1 psi = 6.895 kPa

specimens in this research program. Based on the theory presented by Galati et al. (2003b), Galati developed a computer program to predict the strength of the walls used in this research program. The experimental and theoretical results can be compared in Table 5.5. Also listed in the table are the corresponding reinforcement indexes for each wall. Figure 5.22 plots the ratio of the experimental pressure to the theoretical pressure versus the reinforcement index. This plot indicates that the theory yields reasonable results in predicting the capacity of the walls. In the worst case, the experimental result was approximately 80% of the theoretical value. At times the theory yields conservative results. The theory suggests that the crushing of the masonry is the primary mode of failure of most of the specimens. During testing, none of the walls failed due to concrete crushing; rather most of the failures were initiated by delamination. This may be due to the slight translation of the top boundary member during testing. This translation could have prevented the crushing of the masonry and allowed the wall to resist an increased

Table 5.5. Theoretical Results

Wall #	Experimental Pressure (psi)	Theoretical Pressure (psi)	Reinforcement Index (ω_f)
1	3.5	3.7	-
2	4.4	3.7	-
3	8.0	6.75	0.1556
4	7.6	6.75	0.1556
5	6.8	6.46	0.2631
6	7.3	6.46	0.2631
7	6.4	5.3	0.1556
8	3.2	3.9	0.2631
9	6.2	6.46	0.2631
10	7.3	6.75	0.1556
11	8.4	7.4	0.2787
12	10.1	7.85	0.4083

Conversion: 1 psi = 6.895 kPa

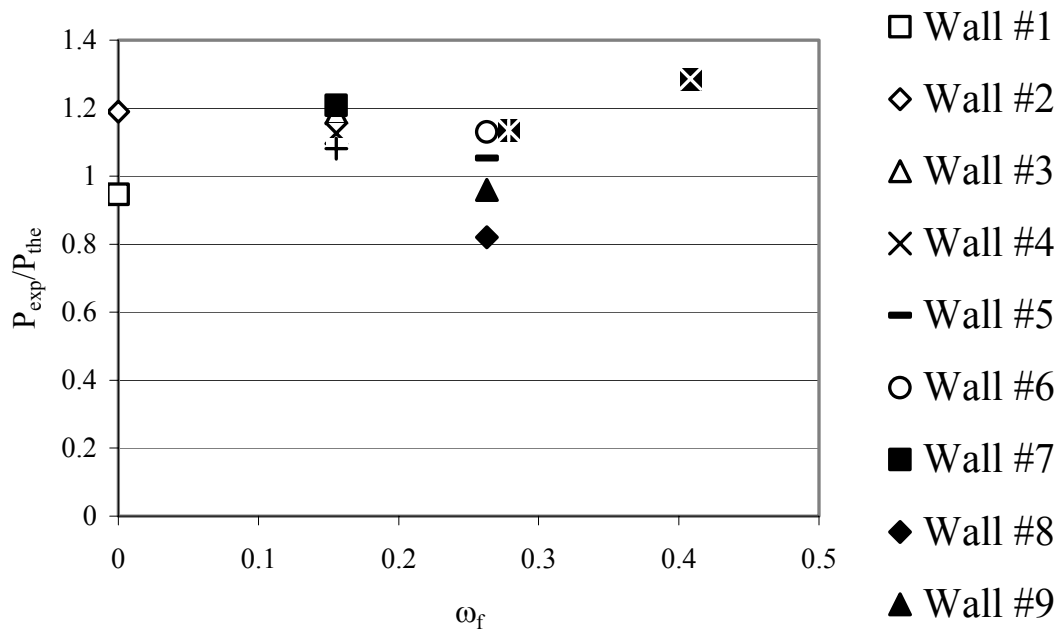


Figure 5.22. Pressure Ratio versus Reinforcement Index

load. Had rotation been fully restrained, concrete crushing may very well have controlled.

To verify the performance of the strengthening systems tested in the lab under blast loads, field blast tests were conducted on two walls. One of the walls was strengthened with GFRP laminates unanchored to the boundary elements, while the other made use of the same reinforcement but included the anchorage detail and shear retrofit. The unanchored wall failed completely at a charge of 4 lb (1.8 kg). The wall in which the FRP was anchored to the boundary elements failed at a charge of 5 lb (2.3 kg). The failure at this charge was only partial. The end stack of blocks comprising the wall began to rotate. In a full scale wall, this rotation would not have occurred due to the fact that the column of blocks would have either been supported by a vertical boundary element or bonded to the next column of blocks. There would not have been an end free to rotate as did the wall in this test program. Despite the rotation, the anchorage detail remained in tack, suggesting that additional capacity could have been obtained had the premature failure not occurred. Even with the rotation, the anchorage clearly provided an increase in capacity over the unanchored wall. The development of continuity between the FRP strengthening material and the surrounding boundary elements is key to increasing a wall's out-of-plane strength and blast resistance for walls of similar slenderness ratios with arching action.

6. CONCLUSIONS

6.1. CONCLUSIONS

The objective of this research program was to evaluate the effectiveness of developing continuity between an FRP strengthened wall system and surrounding RC boundary elements. The effects of bond pattern and variable laminate strip width were also investigated. In an attempt to control shear failure, a shear retrofit detail was developed and included in the construction of several of the walls. The conclusions drawn from this research are as follows:

- Additional capacity is gained by using all of the strengthening methods used in this research with exception to the case of unanchored NSM rods using a stacked bond. This reinforcement technique behaved much the same as the unreinforced wall.
- The development of continuity between the wall system and the surrounding frame provides additional capacity in the out-of-plane direction over the case where the strengthening material is not anchored to the boundary elements, both under static and blast testing.
- Bond pattern, stacked versus running, had limited effect on the out-of-plane strength of the walls.
- The laminate strips tend to hold the wall in tact as it fails, thereby reducing the scatter of debris under static out-of-plane testing. This reduces the risk to the inhabitants of the building.

- Increasing the width of the laminate strips provides even further capacity and allows the wall to fail as a unit, almost eliminating debris scatter under static out-of-plane testing.
- Since no shear problems were observed in this series of tests, the effectiveness of the proposed shear retrofit detail cannot be evaluated.
- The bond characteristics of the various pastes used to apply NSM rods needs to be further investigated to properly evaluate the true strength of the anchorage details.
- The field blast test dynamically validate the laboratory results which suggest that the use of anchorage details or the development of continuity between the wall system and the surrounding RC frame provide further capacity in the out-of-plane direction beyond that gained by strengthening alone.

6.2. FUTURE RECOMMENDATIONS

The following list contains recommendations for future research in the area of out-of-plane loading and blast resistance of unreinforced masonry infill walls.

- Examine an alternate strengthening scheme in which the wall itself is strengthened with laminates and NSM rods are used at the boundary elements for the development of continuity.
- Increase the size of the test specimens to allow for higher slenderness ratios, in which shear may become a controlling failure mechanism with and without arching action.

- Develop a test setup for full scale testing, including fully rigid boundary elements to better reproduce an actual RC framing system.

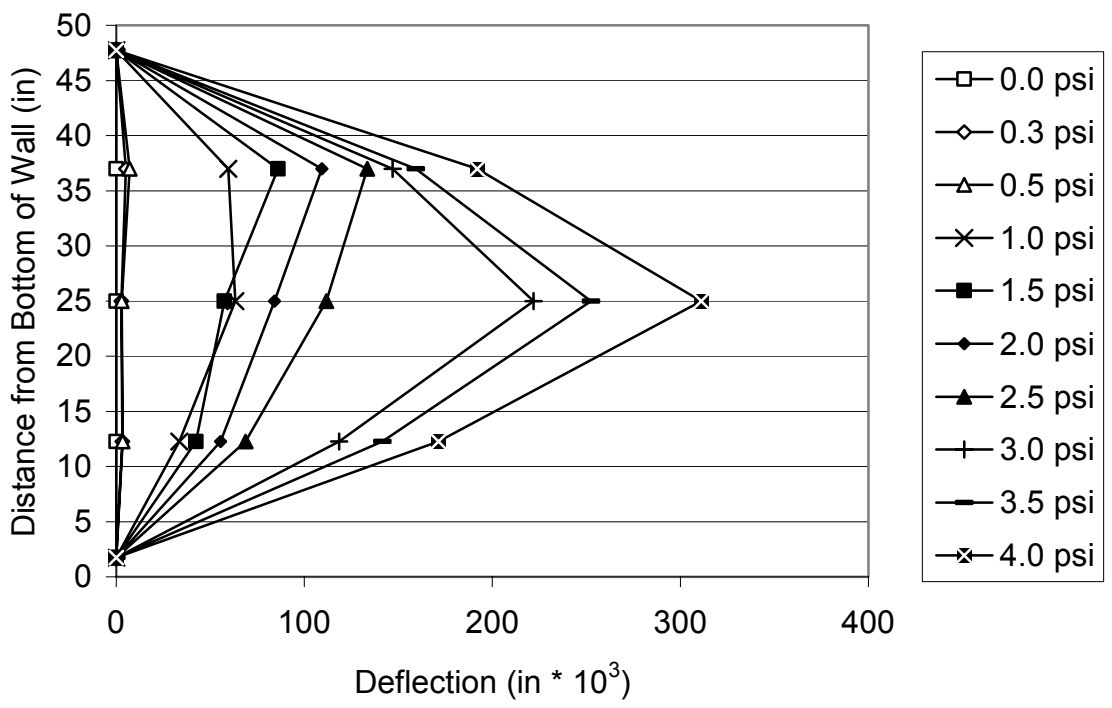
Determine the effects of reinforcement ratio as the head joint spacing increases from 12 in (304.8 mm) to 16 in (406.4 mm) for standard 8 in (203.2 mm) blocks.

APPENDIX A.

TEST DATA

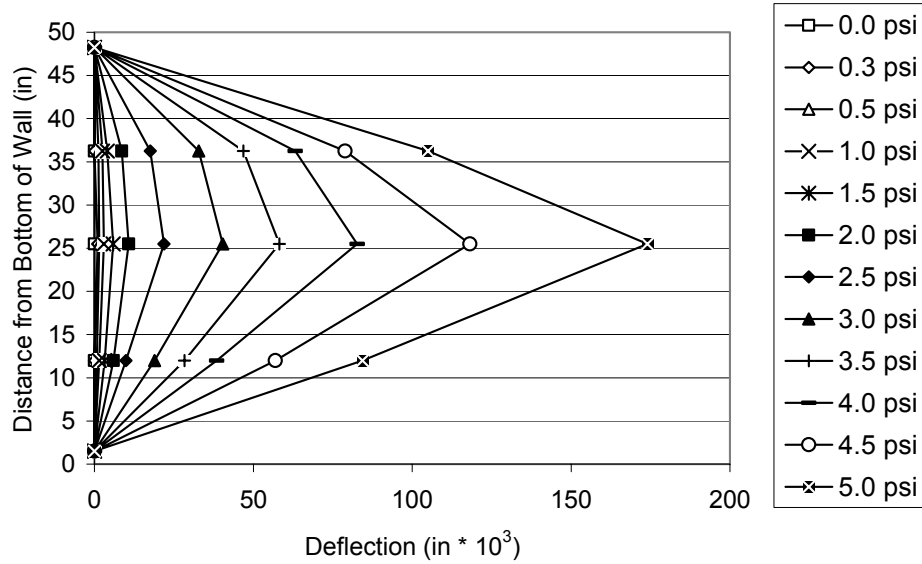
A.1. DEFLECTED SHAPE

Appendix A.1 contains plots of deflection readings at various pressures versus the height of the wall. These plots have been normalized to take into account the slight rotation of the top boundary member that occurred during testing. The deflection plots show the deflected profile of the walls up to the point where the dial gages were removed for safety reasons. It is evident from these plots that arching action is present in the experiment.



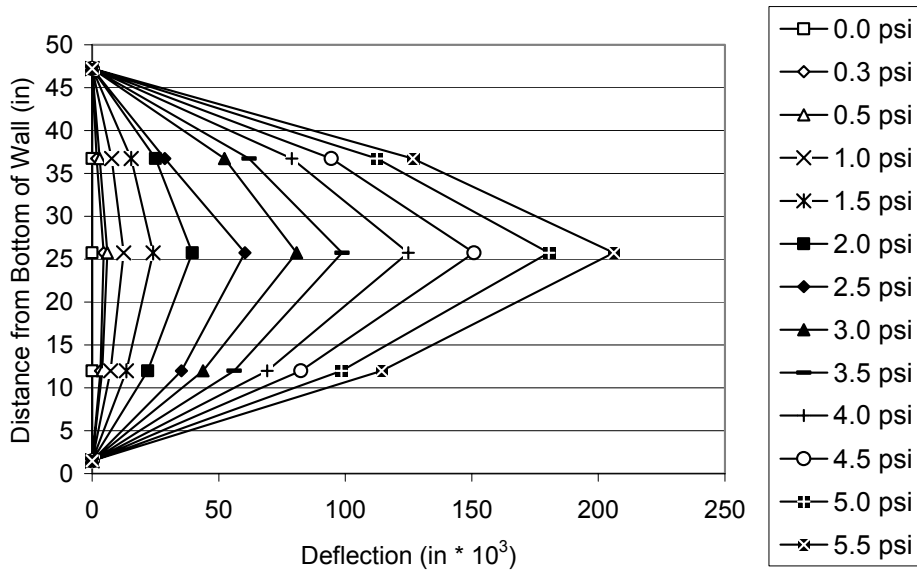
Conversion: 1 in = 25.4 mm

Figure A.1.1. Wall #1 Deflected Shape



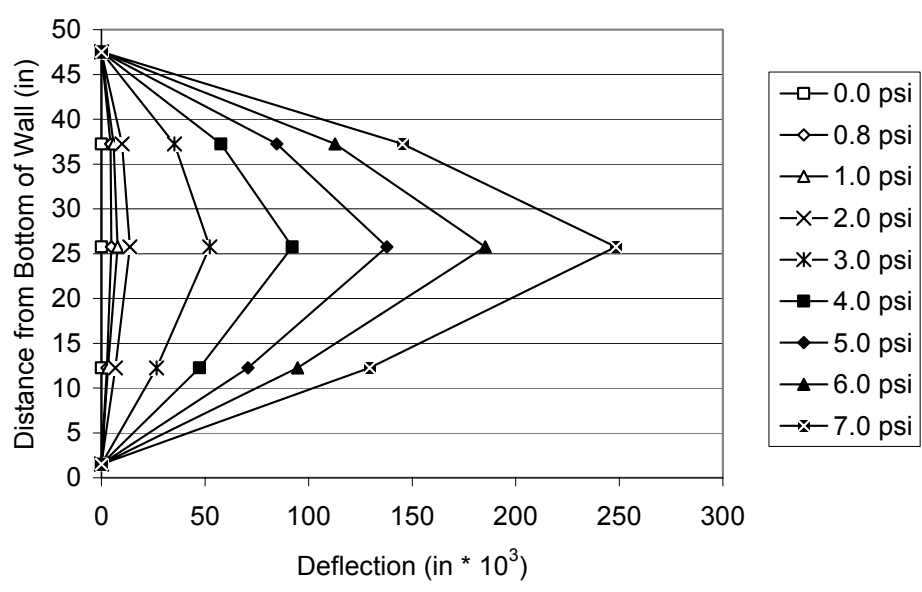
Conversion: 1 in = 25.4 mm

Figure A.1.2. Wall #2 Deflected Shape



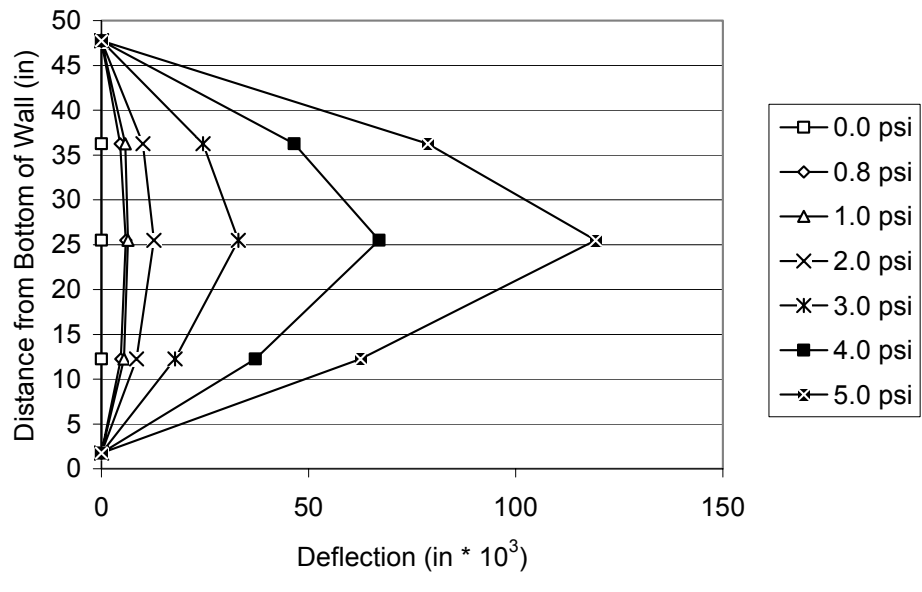
Conversion: 1 in = 25.4 mm

Figure A.1.3. Wall #3 Deflected Shape



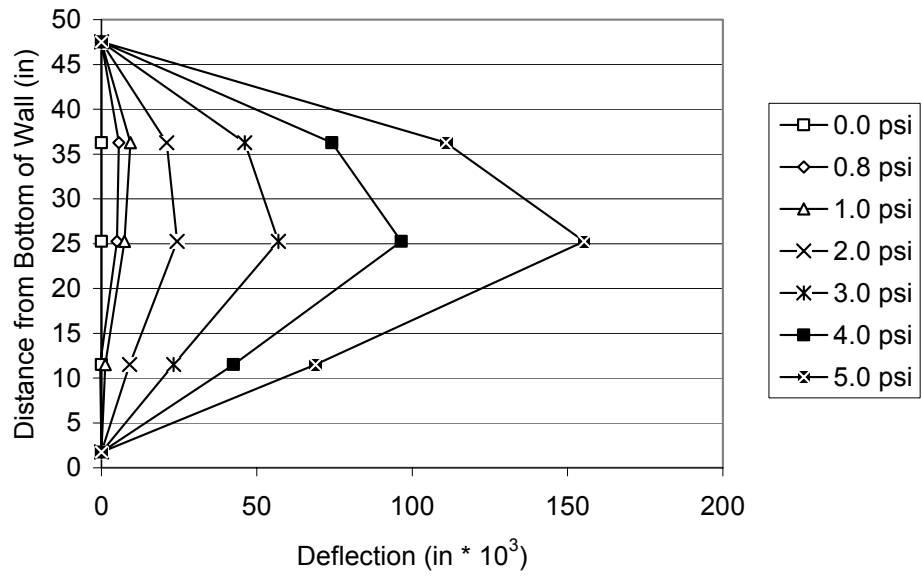
Conversion: 1 in = 25.4 mm

Figure A.1.4. Wall #4 Deflected Shape



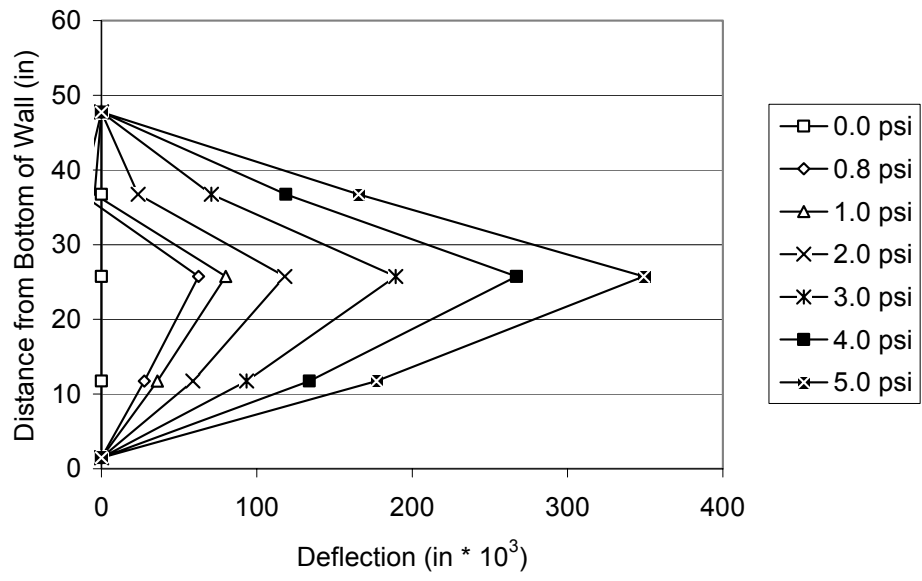
Conversion: 1 in = 25.4 mm

Figure A.1.5. Wall #5 Deflected Shape



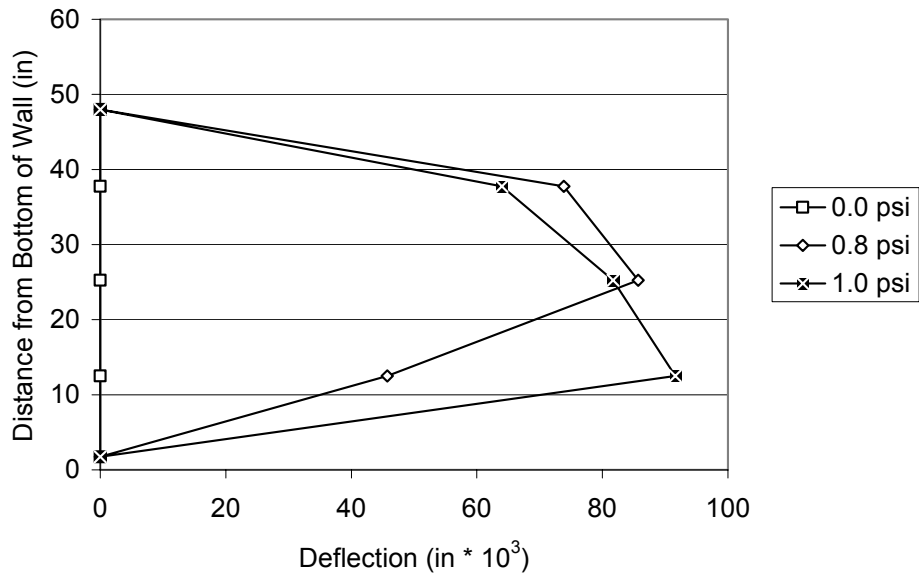
Conversion: 1 in = 25.4 mm

Figure A.1.6. Wall #6 Deflected Shape



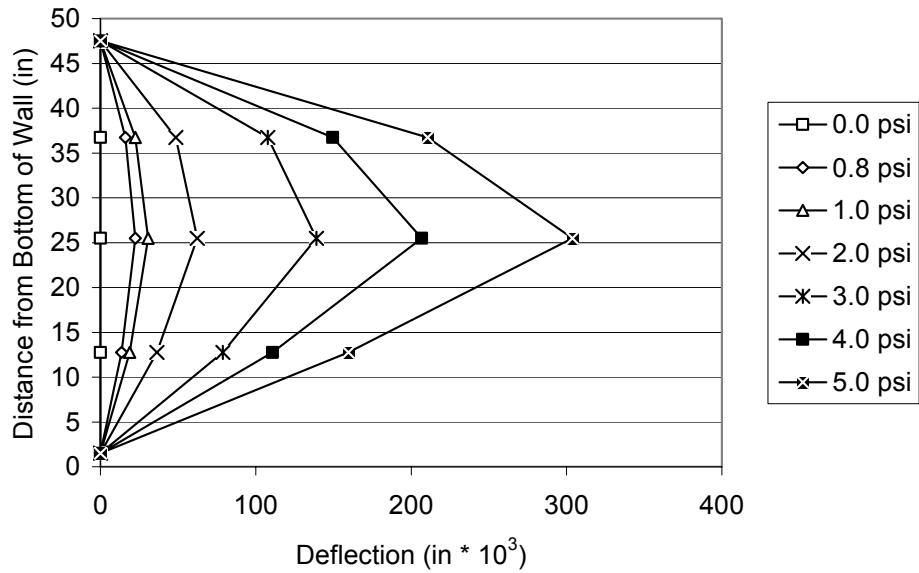
Conversion: 1 in = 25.4 mm

Figure A.1.7. Wall #7 Deflected Shape



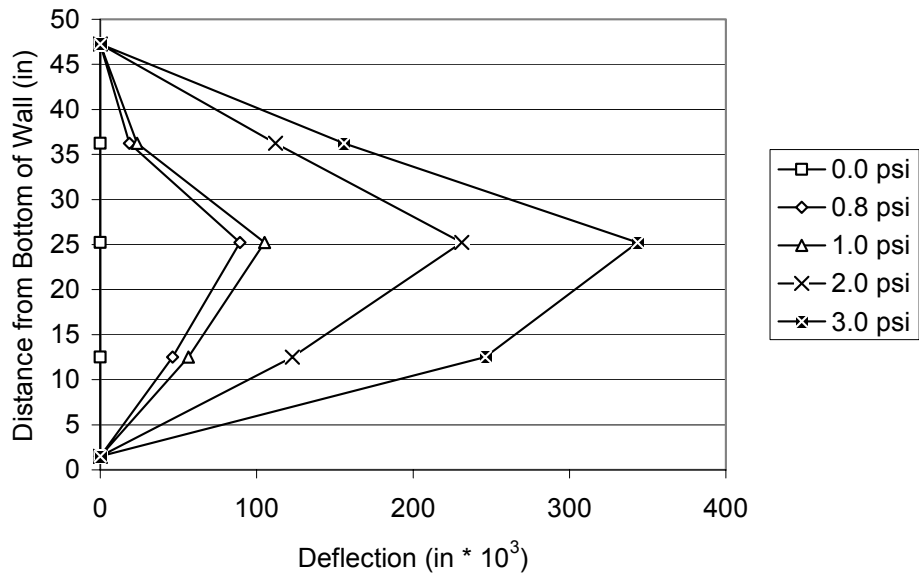
Conversion: 1 in = 25.4 mm

Figure A.1.8. Wall #8 Deflected Shape



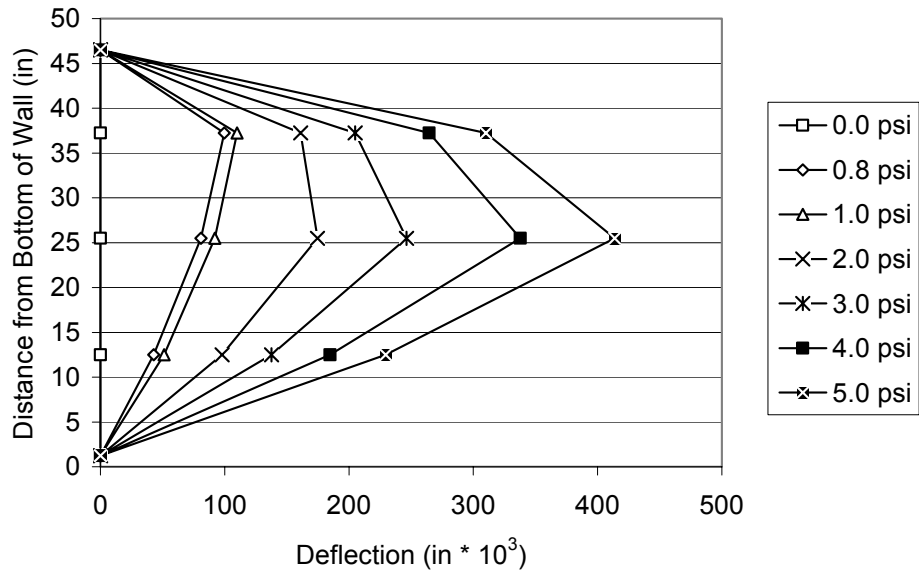
Conversion: 1 in = 25.4 mm

Figure A.1.9. Wall #9 Deflected Shape



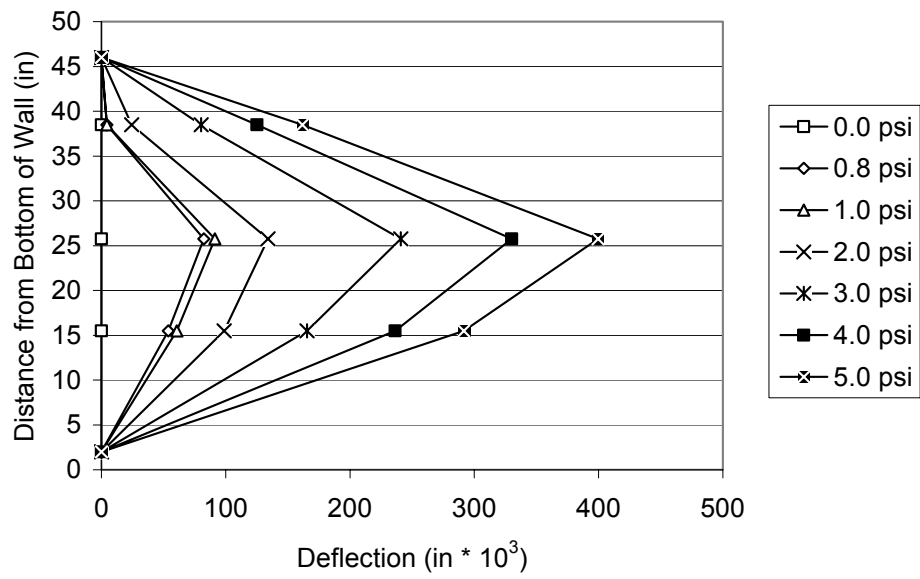
Conversion: 1 in = 25.4 mm

Figure A.1.10. Wall #10 Deflected Shape



Conversion: 1 in = 25.4 mm

Figure A.1.11. Wall #11 Deflected Shape

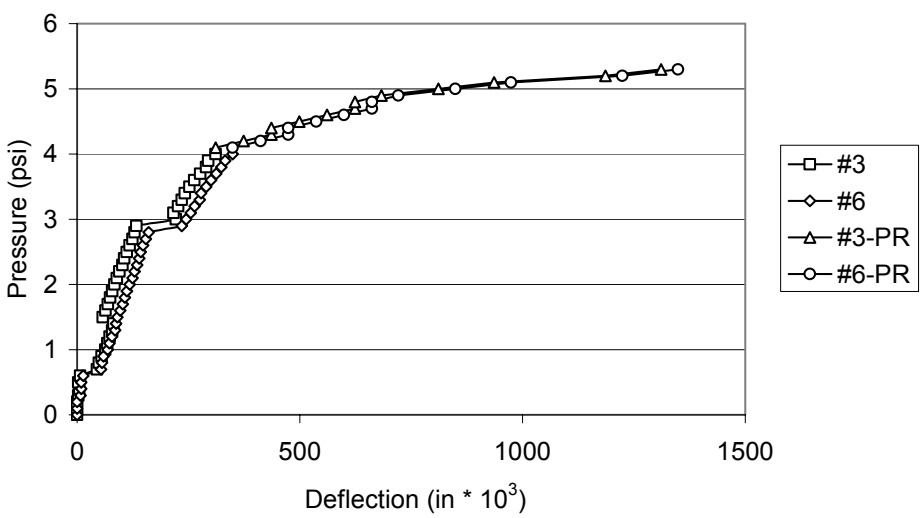


Conversion: 1 in = 25.4 mm

Figure A.1.12. Wall #12 Deflected Shape

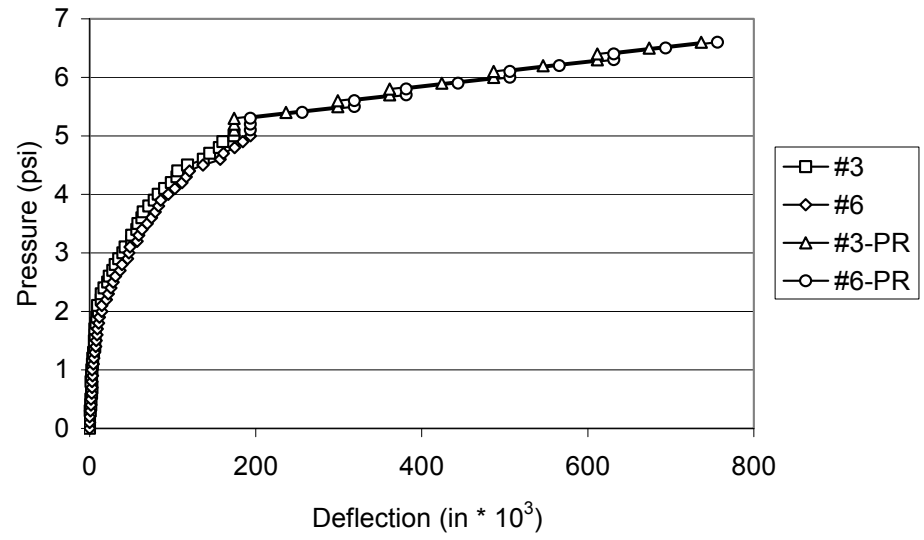
A.2. PRESSURE VS. MIDSPAN DEFLECTION PLOTS

This section contains plots of the pressure versus the midspan deflection. Two curves are shown on each plot representing the two locations on the walls where the midspan deflection was measured. The continuation of the two initial lines is based on the precise ruler (PR) readings recorded by video tape from the time the dial gages were removed until failure of the wall.



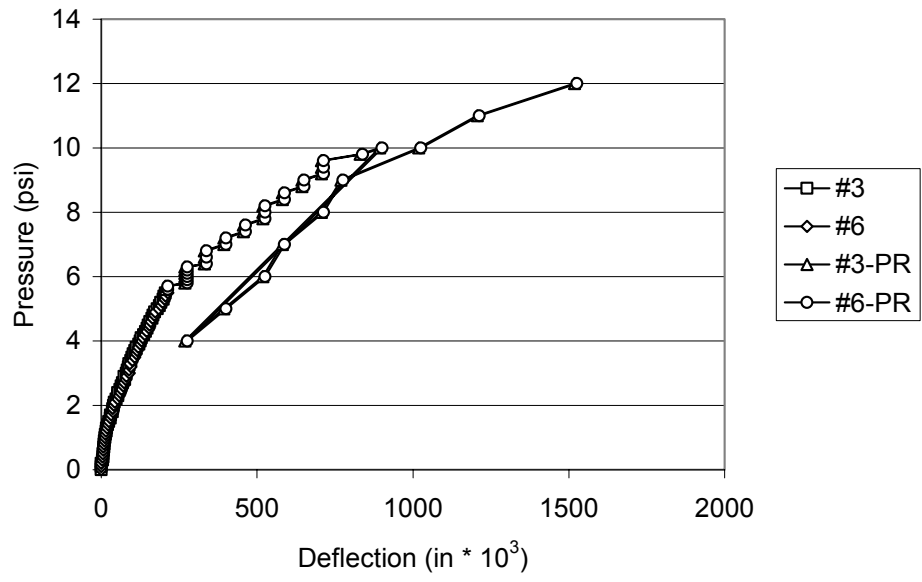
Conversions: 1 in = 25.4 mm, 1psi = 6.895 kPa

Figure A.2.1. Wall #1 Pressure vs. Midspan Deflection



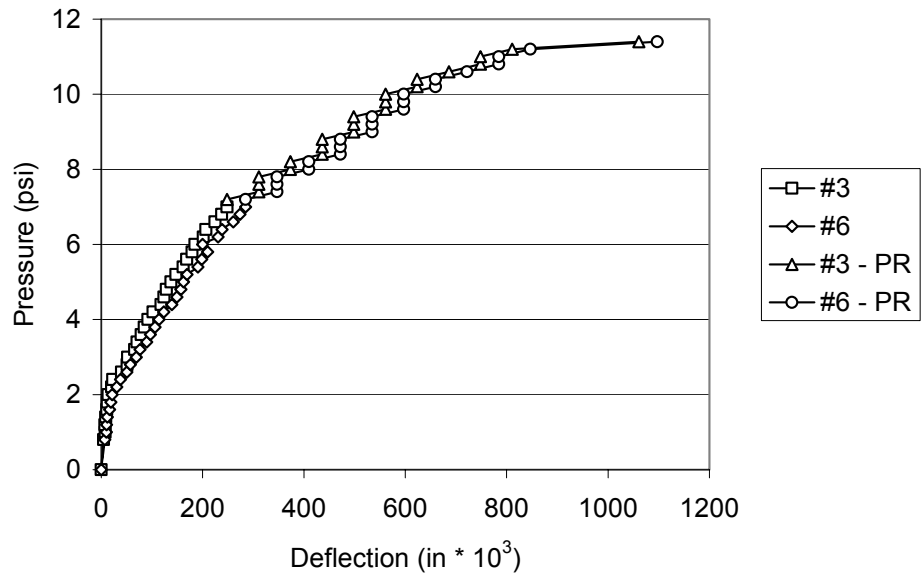
Conversions: 1 in = 25.4 mm, 1psi = 6.895 kPa

Figure A.2.2. Wall #2 Pressure vs. Midspan Deflection



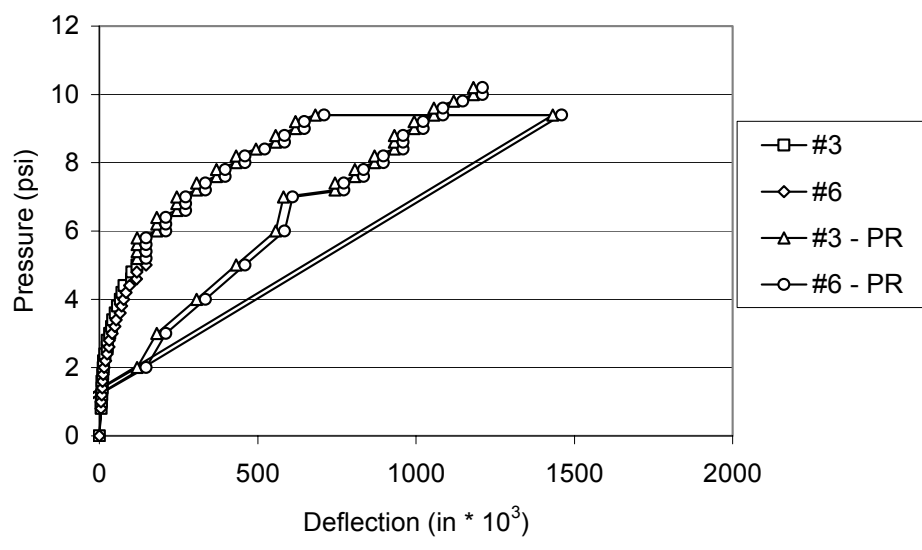
Conversions: 1 in = 25.4 mm, 1psi = 6.895 kPa

Figure A.2.3. Wall #3 Pressure vs. Midspan Deflection



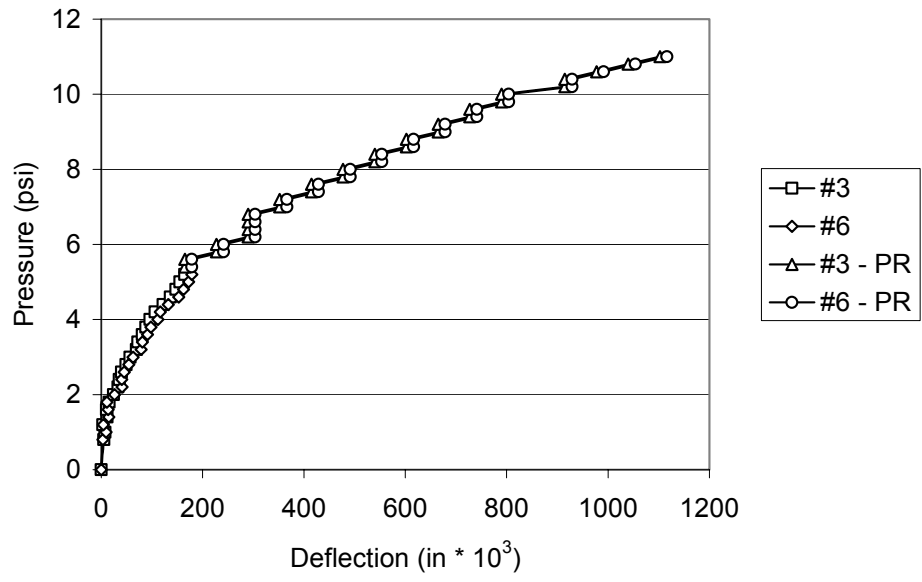
Conversions: 1 in = 25.4 mm, 1psi = 6.895 kPa

Figure A.2.4. Wall #4 Pressure vs. Midspan Deflection



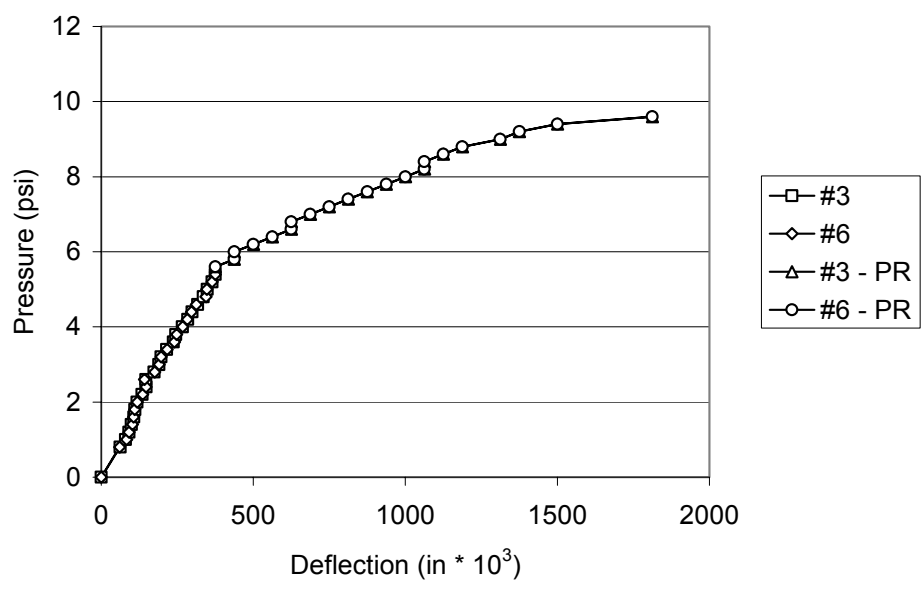
Conversions: 1 in = 25.4 mm, 1psi = 6.895 kPa

Figure A.2.5. Wall #5 Pressure vs. Midspan Deflection



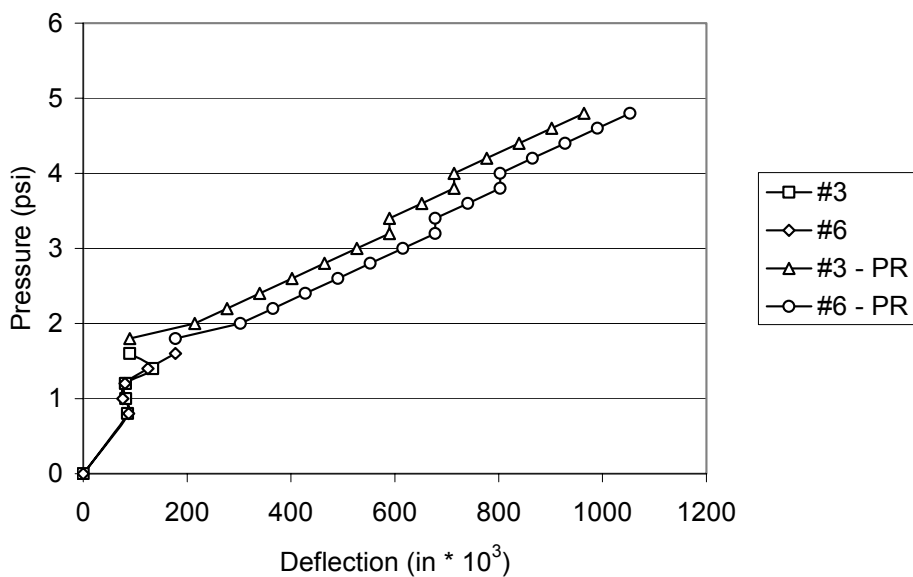
Conversions: 1 in = 25.4 mm, 1psi = 6.895 kPa

Figure A.2.6. Wall #6 Pressure vs. Midspan Deflection



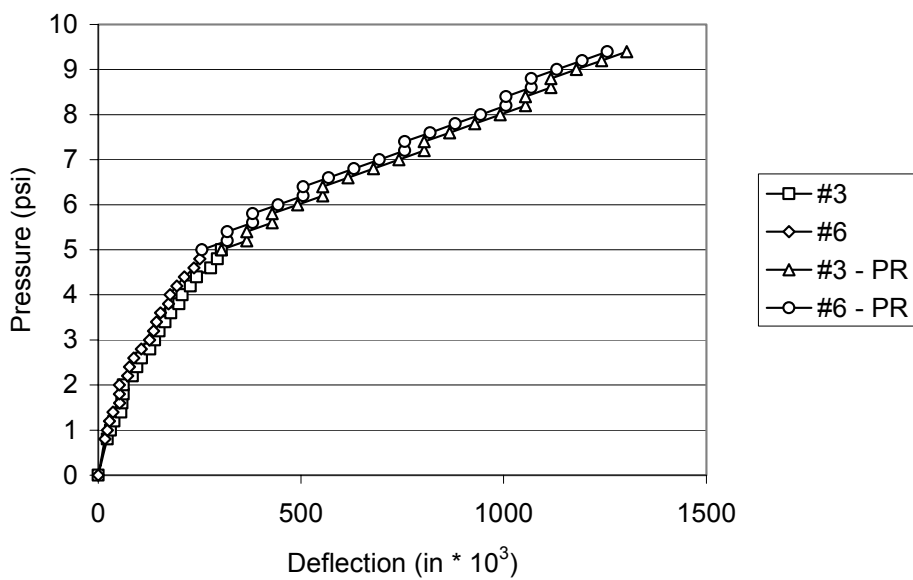
Conversions: 1 in = 25.4 mm, 1psi = 6.895 kPa

Figure A.2.7. Wall #7 Pressure vs. Midspan Deflection



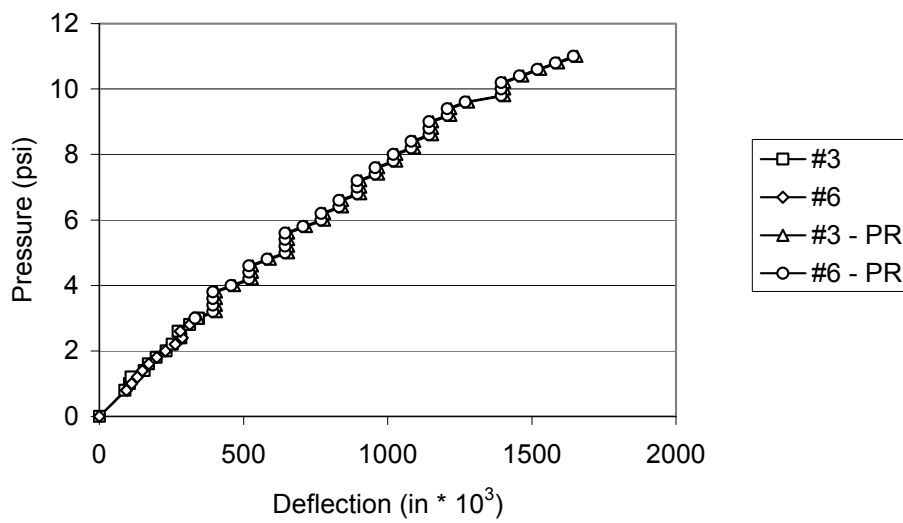
Conversions: 1 in = 25.4 mm, 1psi = 6.895 kPa

Figure A.2.8. Wall #8 Pressure vs. Midspan Deflection



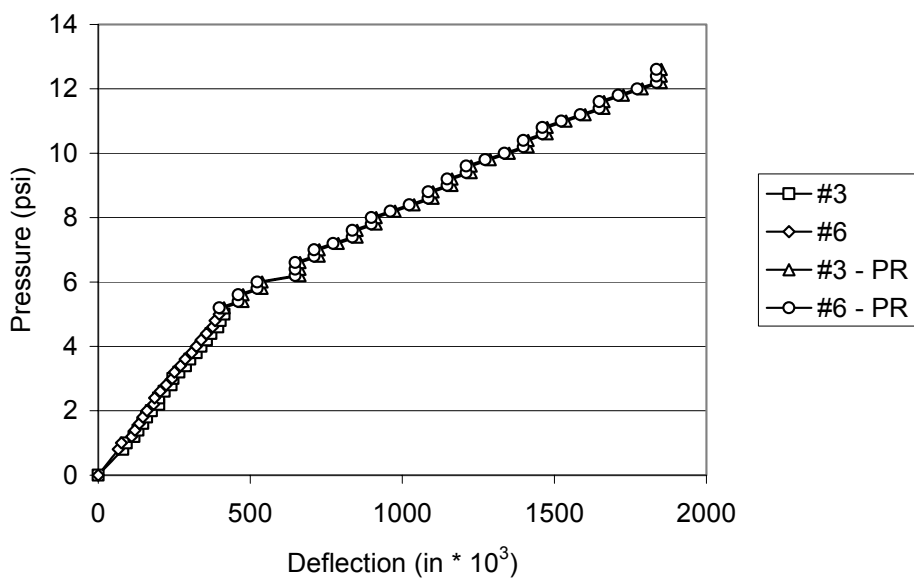
Conversions: 1 in = 25.4 mm, 1psi = 6.895 kPa

Figure A.2.9. Wall #9 Pressure vs. Midspan Deflection



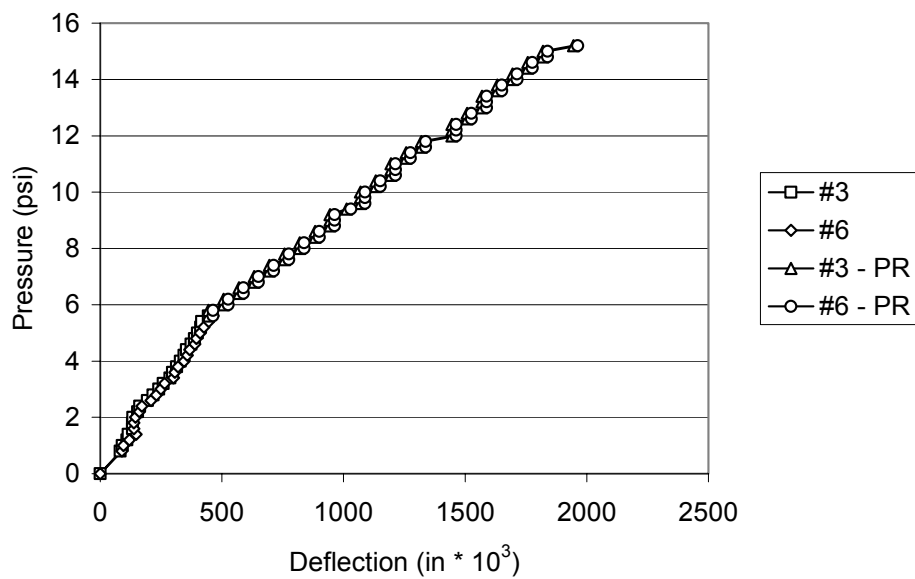
Conversions: 1 in = 25.4 mm, 1psi = 6.895 kPa

Figure A.2.10. Wall #10 Pressure vs. Midspan Deflection



Conversions: 1 in = 25.4 mm, 1psi = 6.895 kPa

Figure A.2.11. Wall #11 Pressure vs. Midspan Deflection

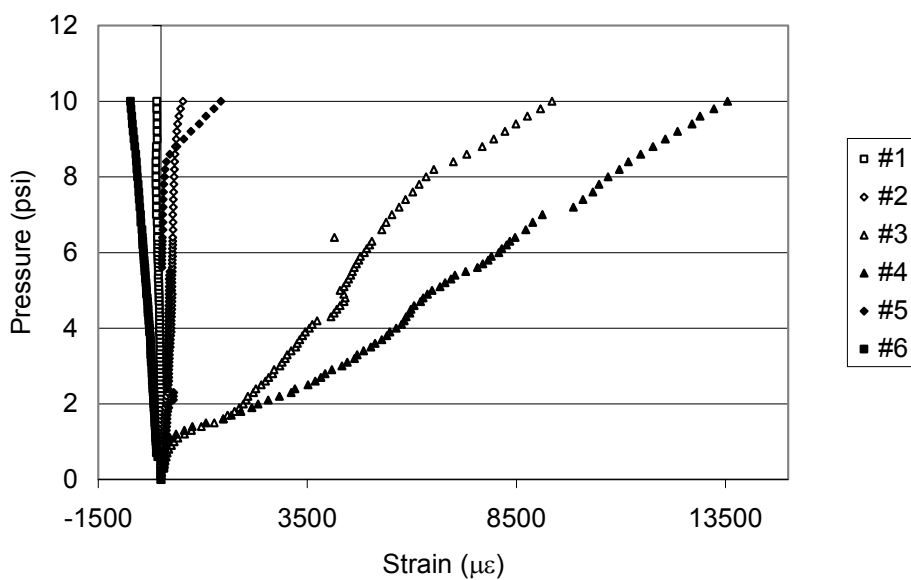


Conversions: 1 in = 25.4 mm, 1psi = 6.895 kPa

Figure A.2.12. Wall #12 Pressure vs. Midspan Deflection

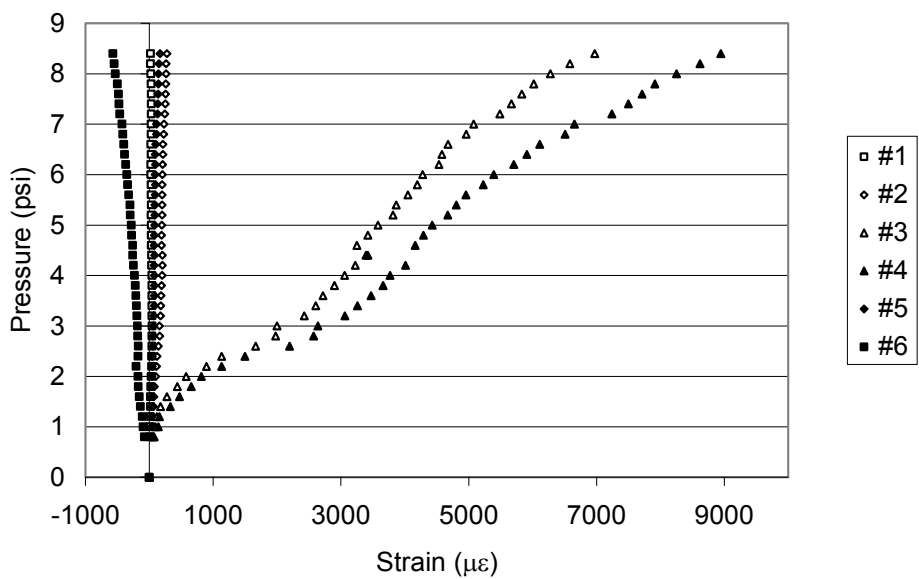
A.3. PRESSURE VS. STRAIN PLOTS

This section contains plots of pressure versus strain. Each plot shows the relationship for each of the six strain gages that were on each wall. The gages were placed on the FRP material at the quarter points of the wall. There were two gages located at midspan, one on each piece of FRP.



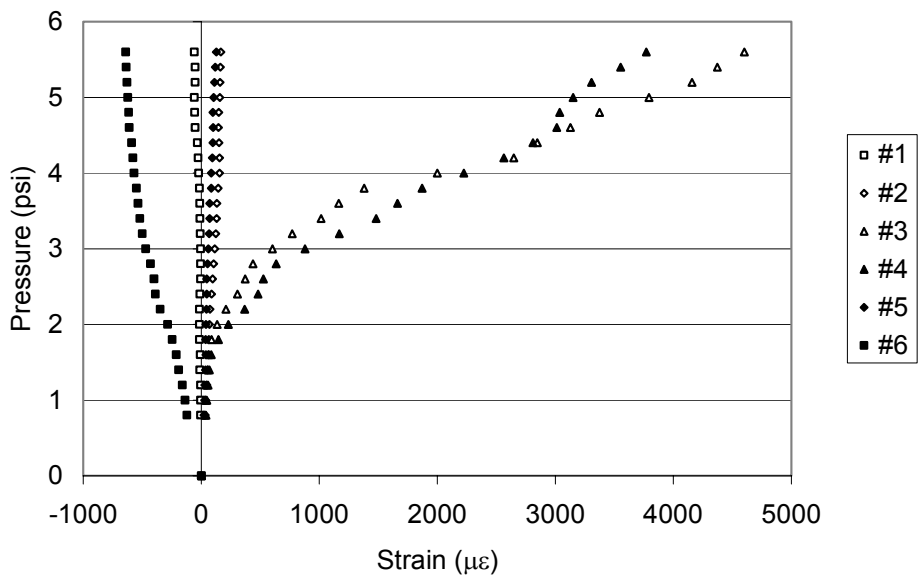
Conversion: 1 psi = 6.895 kPa

Figure A.3.1. Wall #3 Pressure vs. Strain



Conversion: 1 psi = 6.895 kPa

Figure A.3.2. Wall #4 Pressure vs. Strain



Conversion: 1 psi = 6.895 kPa

Figure A.3.3. Wall #5 Pressure vs. Strain

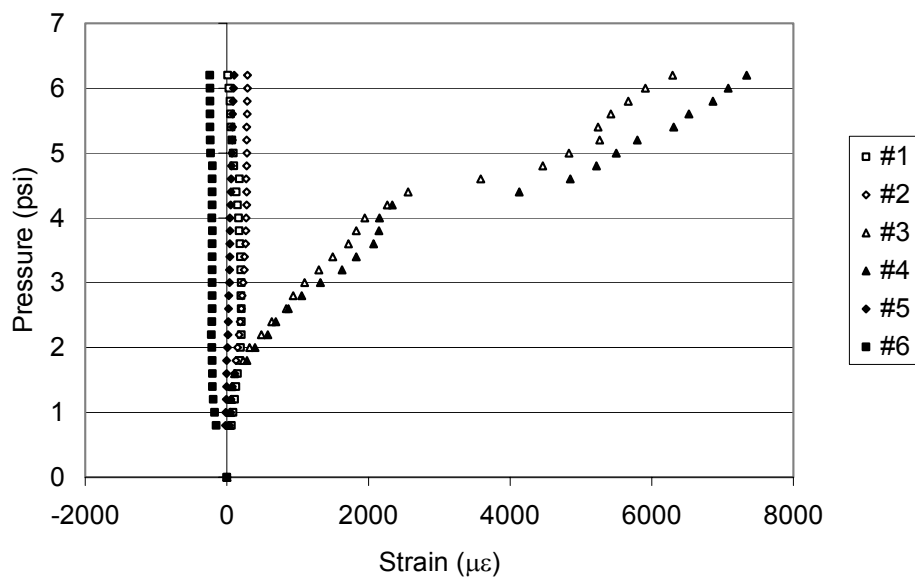


Figure A.3.4. Wall #6 Pressure vs. Strain

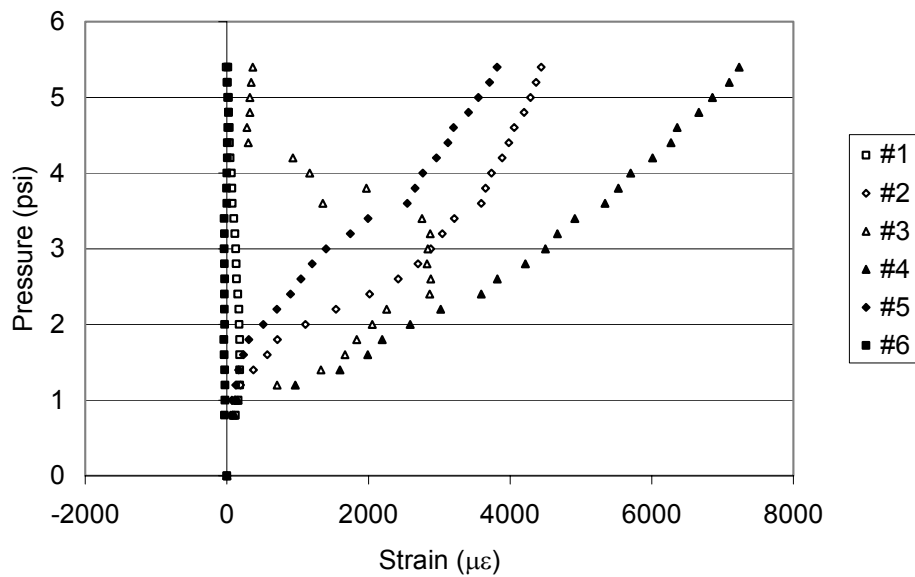
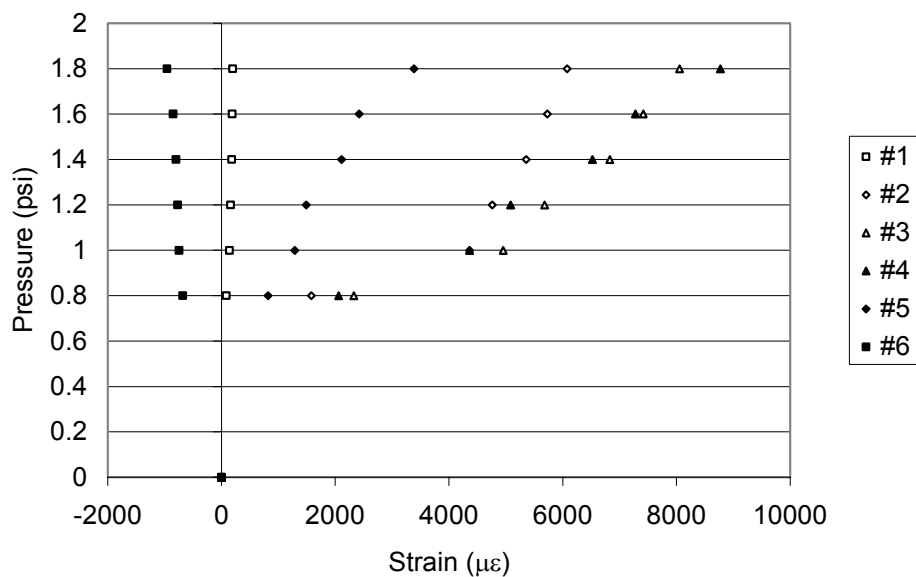
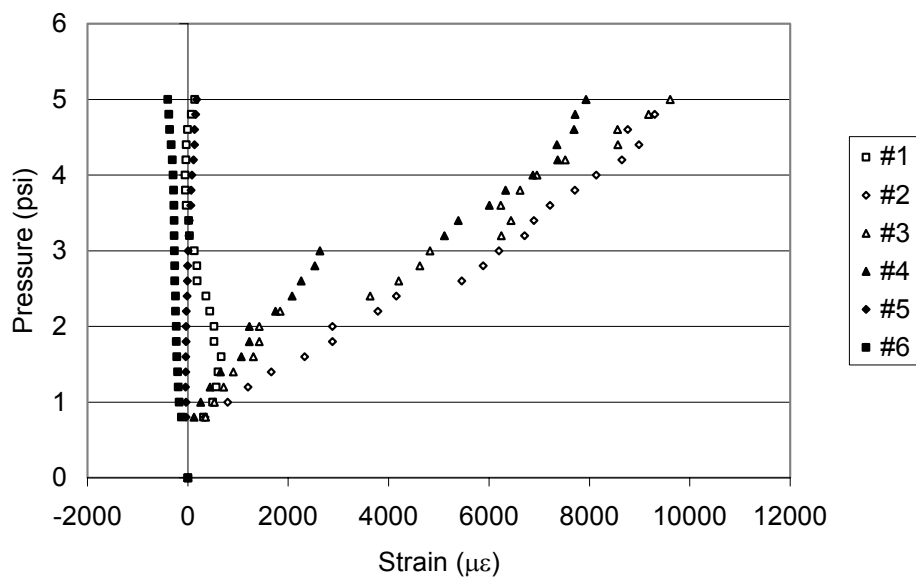


Figure A.3.5. Wall #7 Pressure vs. Strain



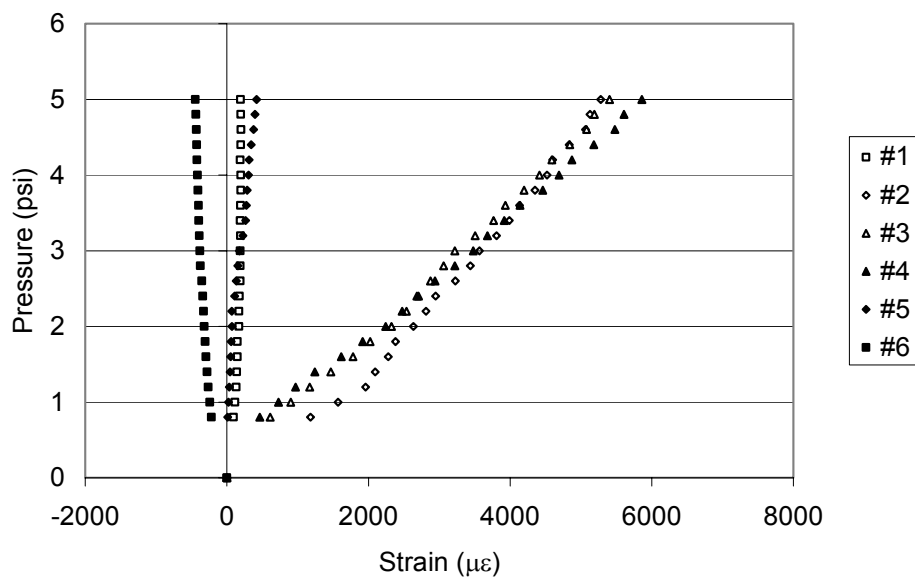
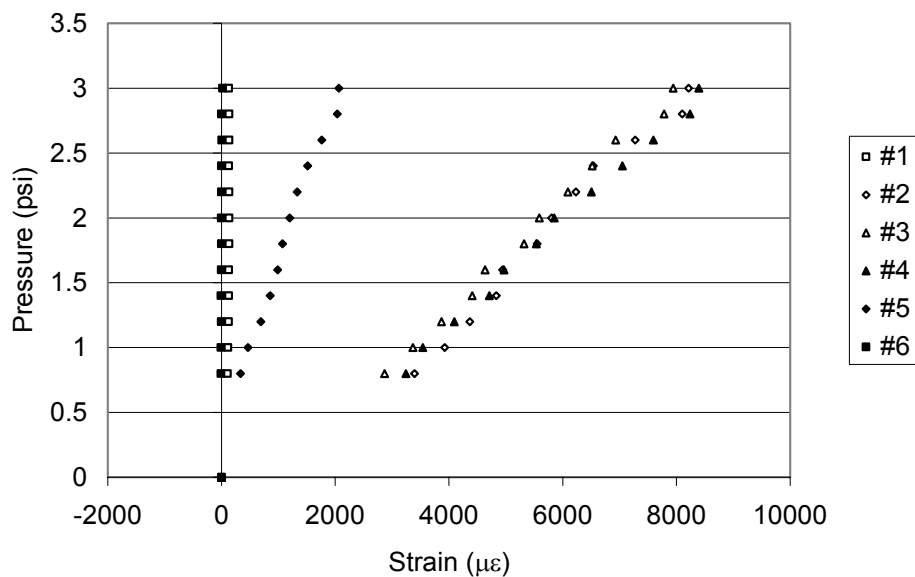
Conversion: 1 psi = 6.895 kPa

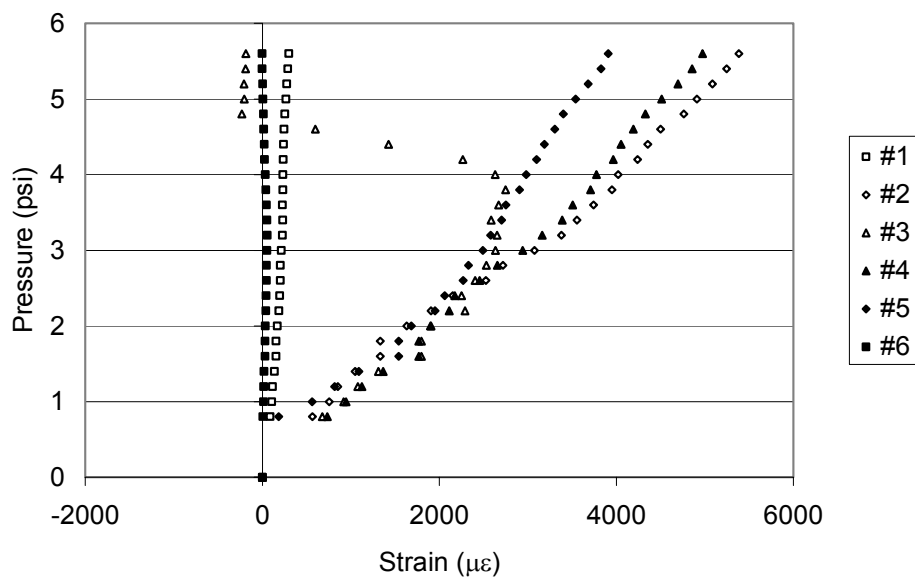
Figure A.3.6. Wall #8 Pressure vs. Strain



Conversion: 1 psi = 6.895 kPa

Figure A.3.7. Wall #9 Pressure vs. Strain





Conversion: 1 psi = 6.895 kPa

Figure A.3.10. Wall #12 Pressure vs. Strain

APPENDIX B.
SAMPLE CALCULATIONS

B.1. CALCULATION OF FACE PRESSURE

$$P_{so} = 6670QR^{-2.5}$$

$$Q = 2lb$$

$$R = 6ft$$

$$P_{so} = 6670 * 2 * 6^{-2.5}$$

$$P_{so} = 151psi(1041kPa)$$

B.2. DEVELOPMENT OF EQUIVALENT UNIFORM PRESSURE

The wall is 48 in (1219 mm) tall. The 7 in (178 mm) directly above the bottom boundary and directly below the top boundary are left unloaded. As a result the wall is only loaded over the center 34 in (864 mm). The maximum shear, V , and maximum moment, M , under these conditions are calculated below where w is the uniform load applied to the wall:

$$V = 34w/2$$

$$V = 17w$$

$$M = 7 * 17w + 1/2 * 17w * 34/2$$

$$M = 263.5w$$

Assuming simply supported conditions, the maximum moment under a truly uniform load, w' , is as follows:

$$M = w' * l^2 / 8$$

$$M = w' * 48^2 / 8$$

$$M = 288w'$$

By equating the maximum moments we can solve for the applied uniform load in terms of the equivalent uniform load:

$$M = 288w' = 263.5w$$

$$w = 1.09w'$$

To obtain the pressure applied to the wall, p , and equivalent pressure, p' , it is necessary to express w in terms of p . p times the width of the area to which the load is applied is equal to w . The airbag left 5 in (127 mm) on each side of the wall unloaded. The uniform loads in terms of the pressures are as follows:

$$w = 26p$$

$$w' = 36p'$$

Substituting in, the equivalent pressure is obtained in terms of the applied pressure:

$$26p = 1.09 * 36 * p'$$

$$p' = .663p$$

Example: 5.3 psi measured

$$\text{Equivalent uniform pressure} = .663 * 5.3 = 3.5 \text{ psi (24.1 kPa)}$$

B.3. CALCULATION OF CAPACITY USING SHAPIRO ET AL. (1994)

$$w = \frac{2f'_m}{h/t} R_1 R_2 \lambda$$

$$h/t = 48/4 = 12$$

$$R_1 = 1 \quad \text{no previous cracking}$$

$$R_2 = 0.5 \quad \text{no framing on sides}$$

$$\lambda = 0.0496 \quad \text{based on } h/t$$

$$f'_m = 1350 \text{ psi}$$

$$w = \frac{2 * 1350}{12} * 1 * 0.5 * 0.0496 = 5.58 \text{ psi (38.5 kPa)}$$

B.4. CALCULATION OF REINFORCEMENT INDEX

$$\omega_f = \frac{\rho_f E_f}{f'_m (h/t_m)}$$

For the 2.5 in laminates:

$$E_f = 10500 \text{ ksi}$$

Thickness = 0.0139 in

Therefore:

$$\rho_f = \frac{A_f}{b_m t_m} = \frac{2.5 * 2 * 0.0139}{36 * 4} = 0.00024$$

$$w_f = \frac{0.00024 * 10500}{1.350 * 48 / 4} = 0.1556$$

BIBLIOGRAPHY

- ACI Committee 440 (2002). "Design and Construction of Externally Bonded FRP Systems for Strengthening Concrete Structures (440.2R-02)," American Concrete Institute, Farmington Hills, MI.
- ACI Committee 440 (2001). "Guide for the Design and Construction of Concrete Reinforced with FRP Bars (440.1R-01)," American Concrete Institute, Farmington Hills, MI.
- ASTM C 31/C 31M - 00 (2000). "Standard Practice for Making and Curing Concrete Test Specimens in the Field." American Society of Testing and Materials, West Conshohocken, PA.
- ASTM C 39/C 39M - 01 (2001). "Standard Test Method for Compressive Strength of Cylindrical Concrete Specimens." American Society of Testing and Materials, West Conshohocken, PA.
- ASTM C 109/C 109M - 02 (2002). "Standard Test Method for Compressive Strength of Hydraulic Cement Mortars." American Society of Testing and Materials, West Conshohocken, PA.
- ASTM C 387 - 00 (2000). "Standard Specification for Packaged, Dry, Combined Materials for Mortar and Concrete." American Society of Testing and Materials, West Conshohocken, PA.
- ASTM C 1314 – 02a (2002). "Standard Test Method for Compressive Strength of Masonry Prisms." American Society of Testing and Materials, West Conshohocken, PA.
- Albert, M. L., Elwi, A. E., and Cheng, J. J. R., (2001). "Strengthening of Unreinforced Masonry Walls Using FRPs." *Journal of Composites for Construction*. American Society of Civil Engineers, Reston, VA.
- Angel, R., Abrams, D., Shapiro, D., Uzarski, J., and Webster, M. (1994). "Behavior of Reinforced Concrete Frames with Masonry Infills." Report, Department of Civil Engineering, University of Illinois, Urbana, IL sponsored by the National Science Foundation, Arlington, VA.
- ChemRex[®] (2002). "Concresive[®] 1420, General-purpose gel epoxy adhesive." Shakopee, MN.
- Dafnis, A., Kolsch, H., and Reimerdes, H. (2002) "Arching in Masonry Walls Subjected to Earthquake Motions." *Journal of Structural Engineering*. American Society of Civil Engineers, Reston, VA.

- Dennis, S., Baylot, J., and Woodson, S. (2002). "Response of 1/4-Scale Concrete Masonry Unit (CMU) Walls to Blast." *Journal of Engineering Mechanics*. American Society of Civil Engineers, Reston, VA.
- El-Domiaty, K.A., Myers, J.J., Belarbi, A. (2002). "Blast Resistance of Un-Reinforced Masonry Walls Retrofitted with Fiber Reinforced Polymers." Center for Infrastructure Engineering Studies Report 02-28, University of Missouri – Rolla, Rolla, MO.
- Ettouney, M., Smilowitz, R., and Rittenhouse, T. (1996). "Blast Resistant Design of Commercial Buildings." *Practice Periodical on Structural Design and Construction*. American Society of Civil Engineers, Reston, VA.
- Galati, N., Tumialan, J. G., Nanni, A., and La Tegola, A. (2002). "Influence of Arching Mechanism in Masonry Walls Strengthened with FRP Laminates." Third International Conference on Composites in Infrastructure, ICCI'02, San Francisco, CA.
- Galati, N., Tumialan, J. G., La Tegola, A., and Nanni, A. (2003a). "Out-of-Plane Behavior of URM Walls Strengthened with FRP Systems." Submitted for Publication, Advancing with Composites 2003, "Plast 2003" – Milan, May 6-10, 2003.
- Galati, N., Tumialan, J. G., and Nanni, A. (2003b) "Influence of Arching Mechanism in Masonry Walls Strengthened With FRP Laminates." Submitted to ACI International, January, 2003.
- Hamilton III, H. R. and Dolan, C. W. (2001). "Flexural Capacity of Glass FRP Strengthened Concrete Masonry Walls." *Journal of Composites for Construction*. American Society of Civil Engineers, Reston, VA.
- Hamoush, S. A., McGinley, M. W., Mlakar, P., Scott, D., and Murray, K. (2001). "Out-of-Plane Strengthening of Masonry Walls with Reinforced Composites." *Journal of Composites for Construction*. American Society of Civil Engineers, Reston, VA.
- Hughes Brothers, Inc. (2001) "Glass Fiber Reinforced Polymer (GFRP) Rebar, Aslan 100." Seward, NE.
- Longinow, Anatol, and Mniszewski, Kim R. (1996). "Protecting Buildings against Vehicle Bomb Attacks." *Practice Periodical on Structural Design and Construction*. American Society of Civil Engineers, Reston, VA.
- Masonry Standard Joint Committee (2002). "Building Code Requirements for Masonry Structures," ACI 530-02/ASCE 5-02/TMS 402-02. American Concrete Institute, American Society of Civil Engineers, and The Masonry Society, Farmington Hills, MI, Reston, VA, Boulder, CO.
- Mays, G. C. and Smith, P.D. (1995). Blast Effects on Buildings. Thomas Telford, London.

Shapiro, D., Uzarski, J., Webster, M., Angel, R., and Abrams, D. (1994). "Estimating Out-of-Plane Strength of Cracked Masonry Infills." Report, Department of Civil Engineering, University of Illinois, Urbana, IL sponsored by the National Science Foundation, Arlington, VA.

Tumialan, J. G. (2001). "Strengthening of Masonry Structures with FRP Composites." Doctoral Dissertation, Department of Civil Engineering, University of Missouri – Rolla, Rolla, MO.

Tumialan, J. G., Galati, N., and Nanni, A. (2003). "FRP Strengthening of URM Walls Subject to Out-of-Plane Loads." *ACI Structural Journal*. American Concrete Institute, Farmington Hills, MI. (Accepted for Publication in May-June 2003 Edition)

Tumialan, J. G., Tinazzi, D., Myers, J. J., and Nanni, A. (2000). "Field Evaluation of Unreinforced Masonry Walls Strengthened with FRP Composites Subjected to Out-of-Plane Loading." Proceedings of the 2000 ASCE Structures Congress, Philadelphia, PA, May 2000.

Velazquez-Dimas, J. I., Ehsani, M. R., and Saadatmanesh, H. (2000). "Out-of-Plane Behavior of Brick Masonry Walls Strengthened with Fiber Composites." *ACI Structural Journal*. American Concrete Institute, Farmington Hills, MI.

Watson Bowman Acme Corp. (2002a). "Wabo[®]MBrace Composite Strengthening System, Engineering Design Guidelines." Amherst, NY.

Watson Bowman Acme Corp. (2002b). "Wabo[®]MBrace EG900, Unidirectional E-Glass Fiber Fabric." Amherst, NY.

